Numerical Sensitivity Experiments of Varying Model Physics on the Structure, Evolution and Dynamics of Two Mesoscale Convective Systems

DA-LIN ZHANG

National Center for Atmospheric Research, Boulder, Colorado*

J. MICHAEL FRITSCH

Department of Meteorology, The Pennsylvania State University, University Park, Pennsylvania

(Manuscript received 22 October 1986, in final form 19 August 1987)

ABSTRACT

The effects of different model physics and different convective and boundary layer parameterization schemes are investigated using an 18-h nested-grid numerical simulation of the mesoscale convective systems (MCSs) that were responsible for the 19–20 July 1977 Johnstown flood. It is found that convective *and* resolvable-scale diabatic processes play crucial yet very different roles in the development and evolution of the MCSs. In particular, latent heat release resulted in development of strong vertical circulations, generation of an upper-level jet streak, formation of pronounced mesoβ-scale surface pressure perturbations, and rapid amplification of the traveling mesoα-scale wave that helped initiate the condensation processes. Resolvable-scale condensations appear to be directly responsible for the generation of a warm-core mesovortex and indirectly for a mesoscale convective complex (MCC). Without resolvable-scale heating, the model only reproduces the propagation of a squall line.

Incorporation of moist downdrafts also had a significant impact on the general evolution of the MCSs by producing important surface perturbations such as mesohighs and outflow boundaries. The role of moist downdrafts in the life cycle of the MCSs appears to be twofold. On one hand, the downdrafts *vertically* stabilized atmospheric columns and removed low-level moisture that otherwise would have been used for mesocyclogenesis and stratiform precipitation. On the other, the downdrafts *horizontally* destabilized the environment through the formation of horizontal temperature and pressure gradients. Specifically, it was found that the cold outflow boundaries over western and southern Pennsylvania helped the development and organization of continued deep convection during the nighttime hours. However, in central Pennsylvania, the warm-core mesovortex was significantly weakened when moist downdrafts were coupled with the updrafts in the convective parameterization scheme.

Inclusion of radiative heating in the surface energy budget tended to produce a conditionally unstable environment favorable for the development and maintenance of deep convection. In general, inclusion of the radiative heating at the surface improved the prediction of timing, frequency and location of convective precipitation. Omission of radiative heating has roughly the same "breaking" effect on the development of the mesovortex as the introduction of the moist downdrafts. It appears that the pronounced diurnal cycle of MCCs is directly related to the thermal cycle of the boundary layer.

Because of sharp and pronounced inhomogeneities in the horizontal moisture distribution, inclusion of virtual temperature instead of just temperature can considerably increase horizontal gradients of geopotential height. Without the virtual temperature effect in the ideal gas law, the model fails to reproduce the warm-core mesovortex and the MCC.

Use of a bulk boundary layer parameterization scheme appears to have a significant effect over mountainous regions. The scheme tends to overestimate the upward energy transport on the upslope side of a terrain feature and underestimate it on the downslope side.

In general, the results indicate that rigorous treatment of model physics is extremely important for simulating the mesoscale convective weather systems and precipitation associated with the Johnstown flood. The results also indicate that successful prediction of "convective" weather systems not only hinges upon the convective parameterization, but also upon the magnitude and distribution of the resolvable-scale latent heat release, and the concurrent development of the diurnal cycle of the boundary layer.

1. Introduction

Despite considerable progress in the development and improvement of numerical models during past decades (see review paper by Anthes, 1983), the ability to predict mesoscale convective systems (MCSs) and

* The National Center for Atmospheric Research is funded by the National Science Foundation.

Corresponding author address: Dr. Da-Lin Zhang, Mesoscale and Microscale Meteorology Division, NCAR, P.O. Box 3000, Boulder, CO 80307-3000.

their precipitation still remains poor. It has been noted that even when the forecast of large-scale circulation and pressure patterns is essentially correct, mesoscale processes often produce embedded "weather" features that depart significantly from the expected large-scale conditions (Sanders, 1979; Charba and Klein, 1980). Recently, there appears to be some agreement that adequate parameterizations of deep convection and the planetary boundary layer (PBL) may be two of the most important components in the improvement of the prediction of mesoscale "weather" events. In particular, in an assessment of the performance of the Limited-area Fine-mesh Model[1] (LFM), Bosart (1980) indicated that the National Meteorological Center (NMC) convective parameterization scheme seemed to have severely damaged the quality of the quantitative precipitation forecasts (QPFs). Correspondingly, in an analysis of the warm-season QPF problem, Heideman (1986) found large sensitivities of the precipitation forecasts to rather arbitrary changes in threshold values of the NMC convective parameterization. Furthermore, many theoretical and numerical studies have shown that model predictions of atmospheric circulations are very sensitive to the magnitude and vertical distribution of convective heating (e.g., Koss, 1976; Anthes and Keyser, 1979; Sardie and Warner, 1983). Thus, it appears that the manner in which the effects of moist convection are introduced into model predictive equations may be crucial to obtaining successful predictions of mesoscale precipitating systems.

The importance of the PBL processes in the development and decay of many types of mesoscale convective weather systems has also been increasingly realized during the past decade (e.g., Ogura and Chen, 1977; Pielke, 1984; Benjamin and Carlson, 1986). This is because the large vertical fluxes of heat, moisture and momentum produced by the PBL processes have a significant effect on the energy supply for the PBL-rooted convective storms. In fact, numerous observational and numerical studies revealed that when meso- or larger-scale dynamical forcing (e.g., strong positive vorticity advection, thermal advection and/or frontal lifting) is weak, the formation and intensification of convective storms are very sensitive to the development of the daytime mixed layer (see Doneaud et al., 1983; Garrett, 1982).

A basic difficulty in adequately parameterizing the aforementioned physical processes in terms of resolvable-scale information is that subgrid-scale convective and turbulent eddies have too wide of a range of complicated scale interactions (i.e., from molecular to mesoβ or mesoα scale) and their effects on the atmospheric circulation vary considerably, depending upon geographic location, season, time of day, large-scale environment, and location within the convective systems. At the present time, it is still not known to what extent these different subgrid-scale processes can be determined from specific resolvable-scale variables. For instance, Rosenthal (1979) noticed that simulated hurricane development is significantly affected when convective parameterization details are changed. Ceselski (1973) observed that varying the vertical latent-heating functions in a primitive equation model produced different magnitudes and distributions of ascending motion, vorticity and static energy associated with the evolution of a Caribbean easterly wave. Moreover, Zack et al. (1985) found pronounced differences in the mesoα scale circulation and precipitation patterns when different convective parameterization schemes were applied. Nevertheless, many numerical studies have demonstrated skill in simulating some observable features of MCSs (e.g., Mahrer and Pielke, 1977; Anthes et al., 1982; Perkey and Maddox, 1985). These studies suggest that successful prediction of the different types of mesoscale convective weather systems may hinge upon closure assumptions, physical processes included in the parameterization, detailed terrain forcing, quality of initial conditions and model resolution of the internal structure of the convective systems and the planetary boundary layer.

The investigation presented in this paper focuses on two of the previously mentioned components: 1) the impact of different model physics on the structure and dynamics of simulated MCSs; and 2) the effects of using different convective and boundary layer parameterization schemes. For the purposes of this investigation, an 18-h simulation of two MCSs (a squall line and a mesoscale convective complex) responsible for the 19–20 July 1977 Johnstown, Pennsylvania flash flood (hereafter referred to as the Johnstown MCSs) was utilized as a control run (see Zhang and Fritsch, 1986a for details). Nine sensitivity experiments were conducted by changing certain physical parameters while holding all other model conditions the same as that in the control simulation. The physical parameters examined include (i) diabatic heating; (ii) convective heating versus resolvable-scale condensation; (iii) parameterized moist updrafts and downdrafts; (iv) Fritsch/Chappell (1980) versus R. A. Anthes/H. L. Kuo (Anthes et al., 1987) type of convective parameterization; (v) surface heating and bulk PBL formulation; and (vi) virtual temperature in the ideal gas law. The model's sensitivity to various mesoscale initial conditions for the same case study has been discussed in another paper by Zhang and Fritsch (1986b). In the next section, the Pennsylvania State University/National Center for Atmospheric Research (PSU/NCAR) mesoscale model used for this study and the control simulation are briefly described. Section 3 presents the design of the experiments. Section 4 contains comparisons of the different experimental simulations to the control case. Discussions of the model results and con-

[1] The Limited-area Fine-mesh Model is run operationally, twice daily, at the National Meteorological Center in Suitland, MD.

cluding remarks are given in sections 5 and 6, respectively.

2. Model description and control simulation

In order to improve the simulation of the mesoβ scale structure and evolution of MCSs, the PSU/NCAR mesoscale model originally developed by Anthes and Warner (1978) has been modified, and now includes the following features for the present study:

- two-way interactive nested-grid procedure (Zhang et al., 1986);
- modified version of the Fritsch/Chappell (FC, 1980) convective parameterization scheme for the fine-mesh portion (Zhang and Fritsch, (1986a);
- R. A. Anthes/H. L. Kuo (AK) type convective parameterization scheme for the coarse-mesh portion (Anthes and Keyser, 1979);
- Blackadar's multilayer "large-eddy" boundary layer parameterization (Zhang and Anthes, 1982; Zhang and Fritsch, 1986a); and
- virtual temperature effects in the ideal gas law.

The nested grid ratio is 1 to 3 with a fine-mesh length of 25 km and a coarse-mesh length of 75 km. The (x, y, σ) dimensions of the coarse and fine meshes are 39 $\times$ 31 $\times$ 19 and 43 $\times$ 37 $\times$ 19, respectively. The model is initialized at 1200 UTC 19 July 1977. For more details of the model and initial conditions, the reader is referred to Zhang (1985) and Zhang and Fritsch (1986a).

As shown in Zhang and Fritsch (1986a), the Johnstown MCSs occurred in a weak-gradient summertime environment in which the thermodynamics (i.e., large amounts of buoyant energy) dominated the dynamic processes. In general, the 18-h control simulation reproduced fairly well the size, propagation rate and orientation of the squall line and mesoscale convective complex (MCC) that were responsible for the Johnstown flood events. In particular, the simulated evolution of diurnal changes in the boundary layer, thunderstorm-generated outflow boundaries, low-level jets, surface pressure perturbations (e.g., mesoβ scale lows, high, ridges and troughs) and a midtropospheric mesoα scale short wave compare favorably with observational analyses by Hoxit et al. (1978) and Bosart and Sanders (1981). Of particular significance is that the predicted rainfall distribution and magnitude are similar to the observed (see Zhang and Fritsch, 1986a, for the verification). Figure 1 presents a portion of the evolution of the surface features from the control simulation (Exp. CTS) for the purpose of comparing the control-run results to the results of the sensitivity experiments. Note that the initial area of deep convection over Lake Erie (Fig. 1a) becomes elongated into the NE–SW orientated squall line (Fig. 1b) as it propagates into Pennsylvania. By 1800 UTC (Fig. 1c), the squall line has intensified and separated from the original convective system (hereafter termed the pre-MCC). In addition, a mesohigh had developed in association with the squall line, and a distinct mesolow appeared in the same region as the pre-MCC. The squall line diminished after 2100 UTC (Figs. 1d and e); however, the pre-MCC expanded and intensified. The mesolow then propagated eastward with the pre-MCC system. Note that a third region of deep convection and a new mesohigh developed along the western boundary of the outflow from the original MCSs. By 0600 UTC (Fig. 1f), deep and intense convective activity occurred only over western Pennsylvania, Maryland, Delaware and southern New Jersey. Convection over eastcentral Pennsylvania and southeastern New York was relatively shallow and weak.

Figures 1g and 1h compare the predicted 12-h rainfall distribution to the observed distribution obtained from the coarse-resolution hourly rain gauge network. The basic patterns are very similar, although the predicted amounts over northwestern Pennsylvania appear to be very heavy. Since satellite and radar data clearly show that virtually all the precipitation over northwestern Pennsylvania fell within this 12-h period, the predicted precipitation was compared to the Hoxit et al. (1978) analysis of the high-density network of 24-h precipitation amounts. The Hoxit et al. (1978) analysis shows a 100 mm maximum over northwestern Pennsylvania and this agrees very well with the model-predicted values (see also Zhang and Fritsch, 1986a). Note that the orientation of the heavy rainfall axis corresponds to the path of the observed mesolow (see Zhang and Fritsch, 1987).

3. Design of experimental simulations

In order to increase our understanding of the various physical mechanisms that produced the Johnstown MCSs and related heavy rainfall, the following physical processes (nine numerical experiments) are examined.

a. Diabatic heating

Neither convective nor resolvable-scale condensation effects are included (Exp. NDH). Supersaturation is removed in this case, but no latent heating is added into the thermodynamic equation. However, the continuity equation for moisture is still integrated in time and the effect of evaporation on the surface energy budget is also included in order to retain the mass field as similar as possible to the control case. Note that this experiment is different from a purely dry forecast since the moisture effect is included in the virtual temperature computation. The importance of using the virtual temperature in the governing equations is discussed in subsections 3f and 4f. Without the forcing from latent heat release, the model dynamics are only subject to free-wave dispersion in which advective processes dominate the model atmospheric circulation. This

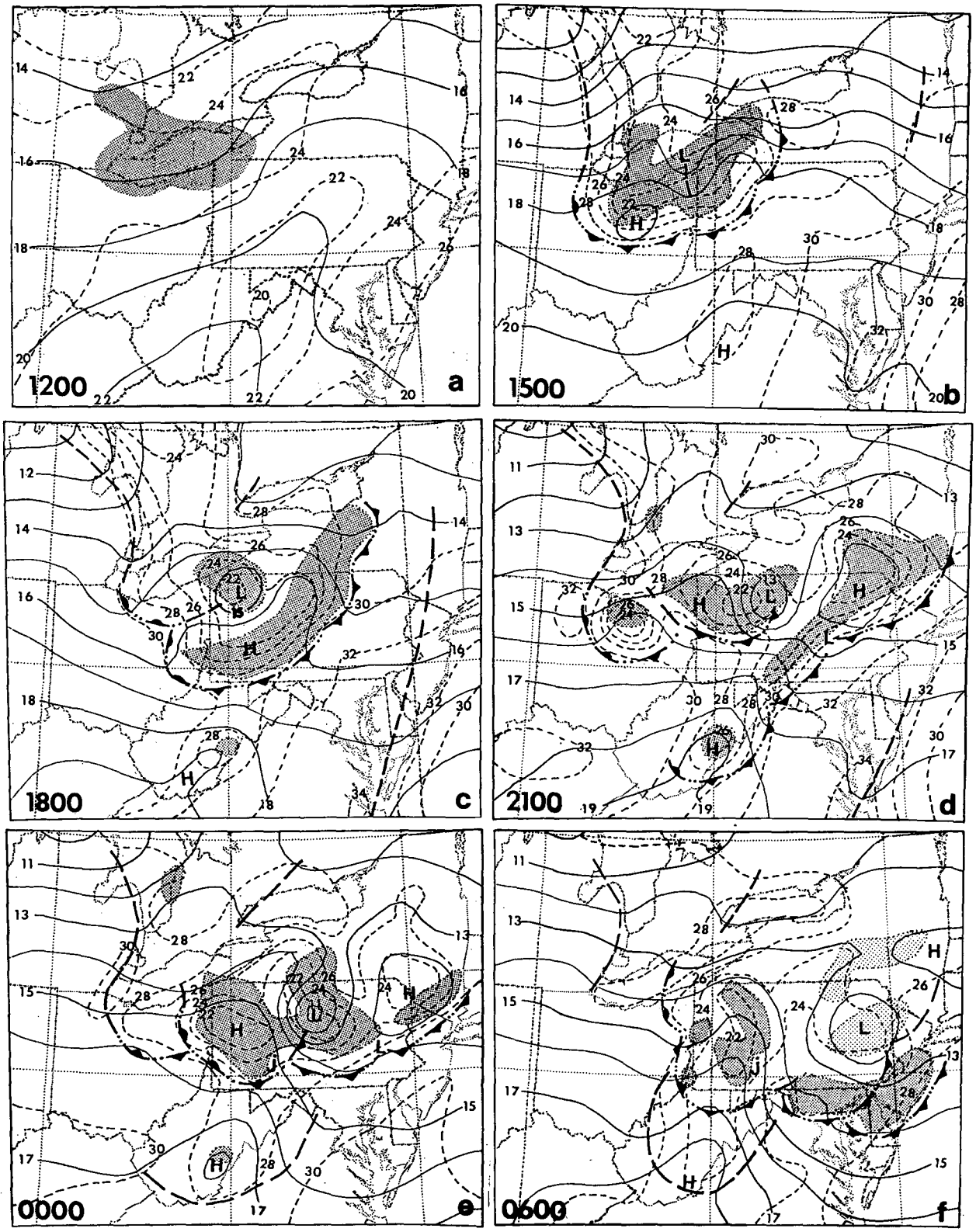

FIG. 1. (a–f) Analysis of sea-level pressure (solid line, mb) and surface temperature (dashed line, °C) for the control simulation. Valid times are shown on each panel. Shading denotes areas of active convection produced by the convective parameterization scheme; dark and light shading indicate relatively deep and shallow convection, respectively. Heavy dashed lines indicate troughs; frontal symbols alternated with double dots denote cool outflow boundaries. (g) Predicted and (h) observed 12-h accumulated rainfall (mm) for the period 1200 UTC 19 to 0000 UTC 20 July 1977.

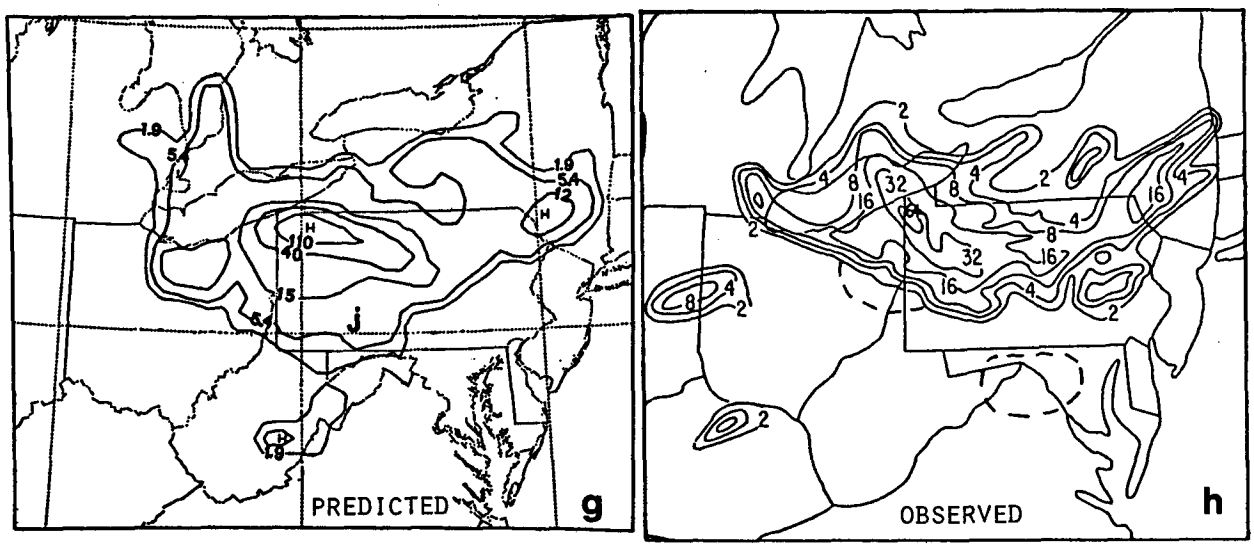

FIG. 1. (*Continued*)

presumably represents the "true" evolution of the meso- and larger-scale environment without the influence of the MCSs. Thus, the purpose of this experiment is to test the hypothesis that without the release of latent heat, the surface pressure perturbations, vertical motion, and amplitude of the midtropospheric short wave would be significantly weaker than that in the control simulation. Another purpose of performing this experiment is to help isolate the significance of individual model physics when comparing Exp. NDH to other sensitivity simulations.

b. Convective versus resolvable-scale heating

In one run (Exp. CPS), only the FC convective parameterization scheme is permitted to produce precipitation, whereas in another run (Exp. RSC), only resolvable-scale condensation is allowed. Conceptually, in a numerical model, the convective scheme provides the effects of precipitating convective clouds that form in conditionally unstable atmospheres, while resolvable-scale latent heating represents the effects of condensation that occurs in saturated atmospheres with favorable mesoscale vertical circulations. Because these two modes of diabatic heating have different distributions and magnitudes in their vertical profiles (see Zhang and Fritsch, 1986a, 1987), they may produce significant differences in the development of MCSs and their associated circulations. Thus, these two experiments are designed to isolate the effects of deep convection and resolvable-scale condensation on the generation of different components of the Johnstown MCSs.

c. Parameterized updrafts and downdrafts

The effects of either parameterized moist downdrafts (Exp. NPD) or updrafts (Exp. NPU) are eliminated. In Exp. NPD, the effects of parameterized downdrafts in the FC scheme are excluded by setting the fractional area occupied by downdrafts (a_d) to zero after a 50% available buoyant energy (ABE) removal requirement is satisfied. Then, the convective effects are computed from

$$\bar{\alpha} = a_u \alpha_u + (1 - a_u)\alpha_e, \tag{1}$$

where α denotes T, q and $\mathbf{V}$, and the subscripts u and e indicate updraft and environmental quantities, respectively. A similar procedure to Exp. NPD is applied for Exp. NPU to exclude the effects of parameterized updrafts, that is,

$$\bar{\alpha} = a_d \alpha_d + (1 - a_d)\alpha_e, \tag{2}$$

where subscript d denotes downdrafts. The purpose of these two experiments is to 1) examine the general response of the development of MCSs in a weak-gradient environment to the parameterized cold downdrafts; and 2) test the hypothesis by Hoxit et al. (1978) that cloud downdrafts played an important role in initiating and focusing the deep convection associated with the MCC over western and southern Pennsylvania.

d. Performance by the AK scheme (Exp. AKC)

Convective effects for both coarse and fine meshes are computed by using the AK convective scheme (Anthes et al., 1987) rather than the FC scheme. As shown in Table 1, several apparent differences exist between these two convective schemes. Since the AK type of convective scheme has been widely used for mesoα or larger-scale simulations of extratropical cyclones, polar lows and MCSs, and also for a number of operational models (e.g., LFM, RAFS, ECMWF),[2]

[2] RAFS is the Regional Analysis and Forecast System at the National Meteorological Center in Suitland, MD. ECMWF refers to models run at the European Center for Medium Range Weather Forecasts.

TABLE 1. Differences between the R. A. Anthes/H. L. Kuo and the Fritsch/Chappell convective parameterization scheme.

	AK	FC
Closure assumption	Moisture convergence	Removal of ABE in a characteristic convective time period
Convective effects	Latent heat releases plus moisture eddy flux	Latent heat release plus eddy fluxes of heat, moisture and momentum
Parameterized elements	Cloud updrafts	Cloud updrafts and downdrafts and compensating environmental vertical motions
"b" parameter	Mean relative humidity in a column	Wind shear and cloud base height
Convective duration	Instantaneous	Convective time scale
Previous applications	Δx = 30–220 km	Δx = 20–25 km

the purpose of applying the AK scheme to the present case is to determine if it is capable of reproducing certain mesoβ-scale features and their associated rainfall patterns. Furthermore, the Johnstown MCSs are more likely to be convectively driven rather than synoptically controlled weather systems. Therefore, comparison of model performance by these two schemes may provide some guidance for developing and/or improving convective parameterization schemes for predicting MCSs that occur in weak-gradient summertime environments.

e. Boundary layer processes

In one experiment, no surface heating is allowed (Exp. NSH) while in another, a one-layer bulk PBL formulation (see Anthes and Warner, 1978) is utilized (Exp. BPL) instead of the Blackadar multilayer PBL package. Note that to properly represent the bulk property of energy and momentum fluxes in Exp. BPL, the vertical sigma levels were redesigned to be uniformly distributed rather than as specified in Zhang and Fritsch (1986a). The purpose of these two experiments is to show the importance of solar energy and a multilayer PBL scheme to the production of the upward transport of moist energy, and also to qualitatively evaluate the diagnostic conclusions by Bosart and Sanders (1981) that the diurnal variation of heat and moisture in the boundary layer had an important impact on the evolution of the Johnstown MCSs.

f. Virtual effect of moisture (Exp. VTP)

Temperature only is employed in the ideal gas law (same as in Anthes and Warner, 1978; Jones, 1977; Gauntlett et al., 1978; Kurihara and Bender, 1980). The use of virtual temperature in the governing equations is considered to be important for simulating MCSs and moist weather systems since the existence of high moisture content in lower levels is essential for producing potential buoyant energy. The subsequent development of convective clouds results in low-level drying and upper-level moistening. This tends to produce the virtual effect of low-level cooling and upper-level heating. Another significant effect of using virtual temperature instead of temperature is in the computation of geopotential height fields. In particular, in spring and summer seasons, when moisture gradients can become very large, horizontal pressure gradients, and therefore winds, can be significantly altered by the distribution of moisture (see Zhang, 1985; Lakhtakia and Warner, 1987). As an example, Fig. 2 shows a comparison of the initial 500-mb height fields computed using both virtual temperature and temperature for the present case. Note that the isoheight contours computed using virtual temperature exhibit a general northward displacement from the heights computed using just temperature, and that the amplitude of the short wave over western Pennsylvania is increased. Furthermore, once model integration starts, advection and terrain-generated asymmetries in the moisture fields (e.g., moist or dry tongues and dry lines) may produce considerable variations in the magnitude and orientation of the horizontal height gradient. Thus, the purpose of this experiment is to quantify the effect of virtual temperature on the generation of some components of the Johnstown MCSs and provide evidence of the important role the moisture plays in both the model dynamics and thermodynamics.

All of these experiments are initialized with the same

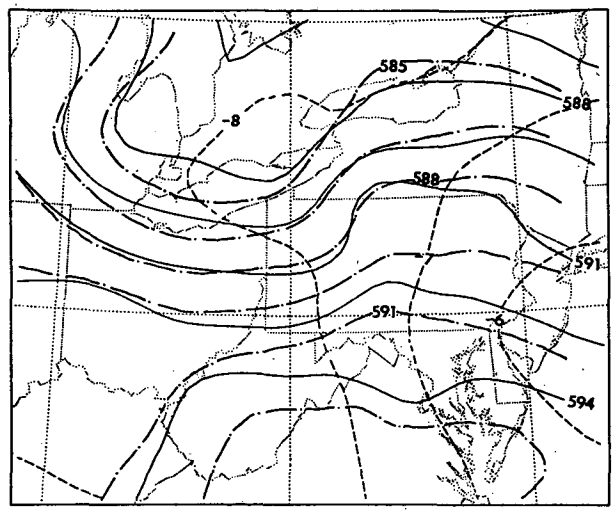

FIG. 2. Comparison of 500 mb heights (dam) computed using virtual temperature (solid lines) with that using just temperature (dot-dashed lines) for 1200 UTC July 1977. Dashed lines are isotherms.

dataset as the control experiment. In the next section, the experimental results of altering the model physics are examined to ascertain how the various physical mechanisms affect the individual components of the Johnstown MCSs.

4. Experimental results

In general, the significance of different model physics to the simulated Johnstown MCSs can be evaluated by examining the structure and/or evolution of a few key parameters: i.e., convective activity, rainfall and surface pressure perturbations. These parameters were found to be good indicators of the model's sensitivity, and a practical measure of the effects of the different physical processes. For most of the experimental simulations, the 6-h and 12-h model results are presented, since several mesoβ scale convective features are at crucial stages at 6-h, while the 12-h simulated distribution of the mesoβ-scale features is very important to determine if the MCSs will continue their development during the evening hours when the boundary layer is cooling. When appropriate, horizontal difference fields between sensitivity and control simulations are shown. Vertical structure and evolution, as well as the large-scale environment, are also displayed to help understand the physical processes responsible for the Johnstown MCSs. In addition, for each experimental simulation, Table 2 lists the central pressure of the major mesolow and the 12-h accumulated convective and resolvable-scale rainfall volume. Detailed descriptions of the results of these experiments are given below.

a. Diabatic heating

Without convective and resolvable-scale condensation effects (Exp. NDH), the model produced a significantly different evolution of the large- and mesoscale weather systems from that which occurred in the control simulation. In particular, in contrast to the rapid development of mesoβ-scale pressure and thermal perturbations in the control case, Exp. NDH shows only minor variations in the pressure and thermal patterns (Figs. 3a–b). The low-level jet (at 900–850 mb) became significantly weaker (not shown); its peak magnitude dropped to less than 30% of that in the control simulation. Moreover, note that without the feedback of the latent heat into the governing system, the precipitation is only a tiny fraction (see Table 2) of the observed and control run precipitation (cf. Figs. 1g, 1h and 3c).

In spite of the obvious effects of the latent heat, it is interesting that the mesoscale troughs in Fig. 3 correspond quite well to the troughs in Fig. 1. For example, the quasi-stationary troughs, labeled A and B in Fig. 3, appear in both simulations and are apparently a result of the differential heating between lake and land surfaces. In fact, in a test simulation without the differential solar heating effects (not shown), these troughs did not appear. In contrast to the quasi-stationary character of troughs A and B, troughs C and D appear to be propagating features and may reflect some type of gravity-wave phenomenon. In particular, it is interesting to note that trough C corresponds extremely well to the position of the squall-line trough that propagates eastward across Pennsylvania (cf. Figs. 1 and 3). Note

TABLE 2. Twelve-hour accumulated convective (V_c) and resolvable-scale (V_r) rainfall volume, and minimum sea-level pressure (P_m) of the major mesolow for each experimental simulation.

	Code	Description of experiment	Parameter investigated	V_c (10^{12} kg)	V_r (10^{12} kg)	P_m (mb)	Integration (hours)
1	CTS	control simulation	—	2.24	1.77	1011	18
2	NDH	neither convective nor resolvable-scale condensation is included	diabatic heating	—	0.09	—	12
3	CPS	convective effects only	convective heating	2.31	—	1015	12
4	RSC	resolvable-scale heating only	resolvable-scale heating	—	3.32	1005	12
5	NPD	cloud downdraft effects are omitted	parameterized downdraft	3.16	1.89	1006	18
6	NPU	only cloud downdraft effects are included	parameterized downdraft	0.97	0.03	—	12
7	AKC	Anthes-Kuo convective scheme is used	convective parameterization	1.02	1.53	1007	12
8	NSH	no surface heating	boundary layer	0.79	1.87	1011	12
9	BPL	bulk PBL formulation	boundary layer	1.95	1.93	1008	12
10	VTP	temperature in gas law	virtual temperature	1.62	0.04	—	12

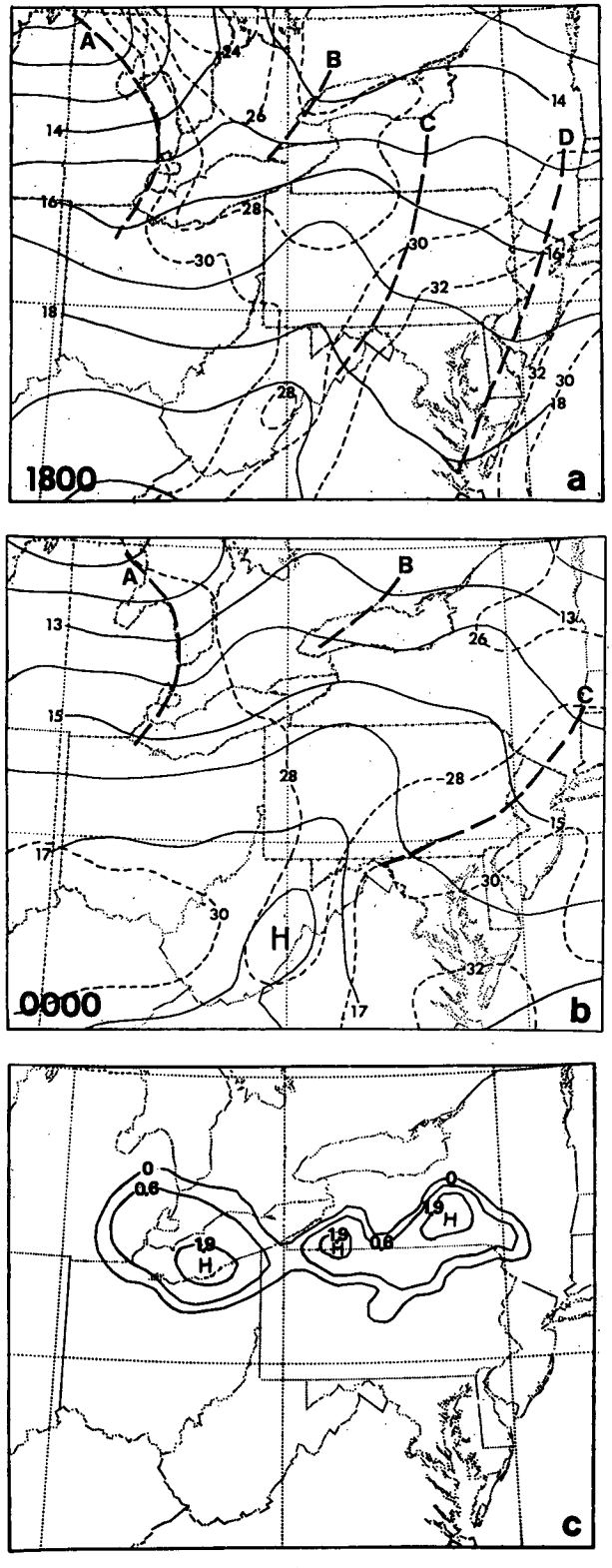

FIG. 3. (a–b) Predicted evolution of sea-level pressure (solid lines, mb) and surface temperature (dashed lines, °C) for Exp. NDH (no diabatic heating). The heavy dashed lines denote pressure troughs. (c) Removed 12-h accumulated rainfall (mm) for the period 1200 UTC 19 to 0000 UTC 20 July 1977.

in Fig. 1 that the precipitation occurs behind the trough. This agrees with internal gravity-wave theory (see Eom, 1975; Uccellini, 1975) and is the subject of further research to understand the organizational and propagation processes of the Johnstown MCSs. The outstanding exception to the general similarity in the pressure patterns from the two simulations is the major mesolow that forms over northwestern Pennsylvania. The development of this low is totally dependent upon latent heat release. A much more thorough examination of the structure and dynamics of this low and associated midtropospheric warm-core vortex is given in Zhang and Fritsch (1987).

Figures 4a and 4b show the observed 700 mb height and thermal fields at model initial time (1200 UTC 19 July 1977) and 12 hours later. Figures 4c and 4d show the same fields for the 12-h forecast from the control simulation and from Exp. NDH, respectively. Clearly, the amplitude of the short wave over Pennsylvania is the weakest for the simulation where latent heat is excluded (Fig. 4d). In fact, the amplitude for Exp. NDH is even weaker than the observed field at the initial time (cf. Figs. 4a and 4d). A similar weakening occurred in the LFM operational 12-h forecast valid at the same time as the simulations shown in Fig. 4. In this forecast, the LFM failed to predict any precipitation over the northeastern United States. It is important to point out that, while the amplitude of the short wave weakened when latent heat was excluded, the amplitude of the large-scale ridge over the western portion of the domain remained essentially the same as in the control run (cf. Figs. 4c and 4d). Since the large-scale ridge region was virtually precipitation free, this indicates that latent heat is responsible for the actual deepening of the wave.

In order to further examine the effects of the diabatic heating on the large (mesoα) scale environment, several difference fields were computed, i.e., the results of Exp. NDH were subtracted from the control simulation. Figure 5 shows the differences in the 12-h forecasts of temperature and vertical motion at low, middle and high levels. The simulated MCSs produced extensive cooling at low levels; this cooling resulted from the parameterized cloud-scale moist downdrafts. Note also that slight warming occurs at some locations along the periphery of the moist downdraft outflow boundary. Presumably, the warming over the northern portion of the domain is the result of mesoscale subsidence driven by the MCSs. The warming over Ohio may be due to subsidence associated with internal gravity wave circulations.

Above the layer of moist downdraft cooling, a deep warm perturbation was produced from roughly 850 to 200 mb. Note that the warming at 500 mb extends well beyond the region of downdraft cooling, (i.e., beyond the area where moist convection occurred) and that the location of maximum warming appears to correspond with the center of the mesovortex. The magnitude of the maximum warming is about the same as

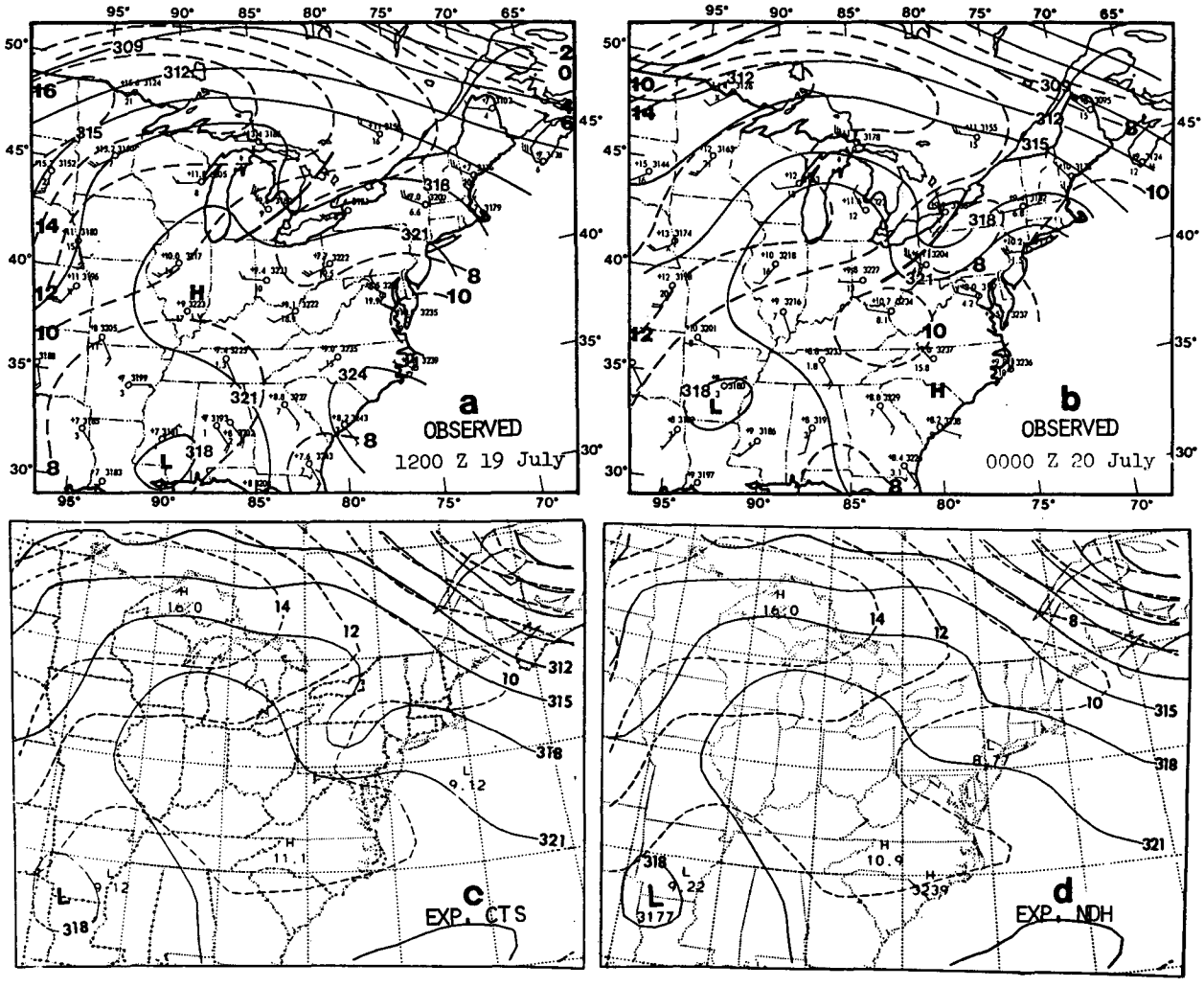

FIG. 4. Comparison of 700 mb heights (dam) and temperature (°C) for (a) the observed conditions at model initial time, 1200 UTC 19 July 1977; (b) observed conditions 12-h later, 0000 UTC 20 July 1977; (c) control simulation valid at 0000 UTC 20 July; and (d) Exp. NDH (no diabatic heating) valid at 0000 UTC 20 July.

that observed in an MCC-generated warm-core vortex that occurred during Pre-STORM experiments (Johnson, 1986). It is of particular interest to consider just how this warming is produced. Near the center of the vortex, Zhang and Fritsch (1987) found that the warm anomaly stems from the transformation of the atmosphere from a subsaturated, conditionally unstable environment with embedded deep convection to a saturated environment with a virtually moist adiabatic lapse rate and resolvable-scale condensation (i.e., saturated mesoscale ascent). Since areas of mesoscale descending motion are also evident in Fig. 5 (right panel), it is possible that some of the warming evident in the left panel resulted from mesoscale compensating subsidence instead of directly by latent heat release. This possibility is examined further in the next section.

In addition to the tropospheric warming and the low-level moist downdraft cooling, an upper-tropospheric layer of cool air was produced by the MCSs (see Fig. 5). This cooling not only extended beyond the area of deep convection, but covered most of the states adjacent to Pennsylvania, as well. Parameterized convective cloud overshooting and evaporation of condensate, in association with adiabatic cooling induced by the resolvable-scale circulation, were responsible for the production of the cool pool. In a case study, Fritsch and Maddox (1981a) found a deep, nearly moist adiabatic layer in the troposphere beneath the cool pool (see Figs. 23 and 24 in Fritsch and Maddox, 1981a). Apparently the broad extent of the cool pool beyond the area occupied by the MCSs is related to the strongly diverging outflow in a *thin* layer above the MCSs (see Fig. 6 and Wetzel et al., 1983).

It is also shown in Fig. 5 that a distinct organized

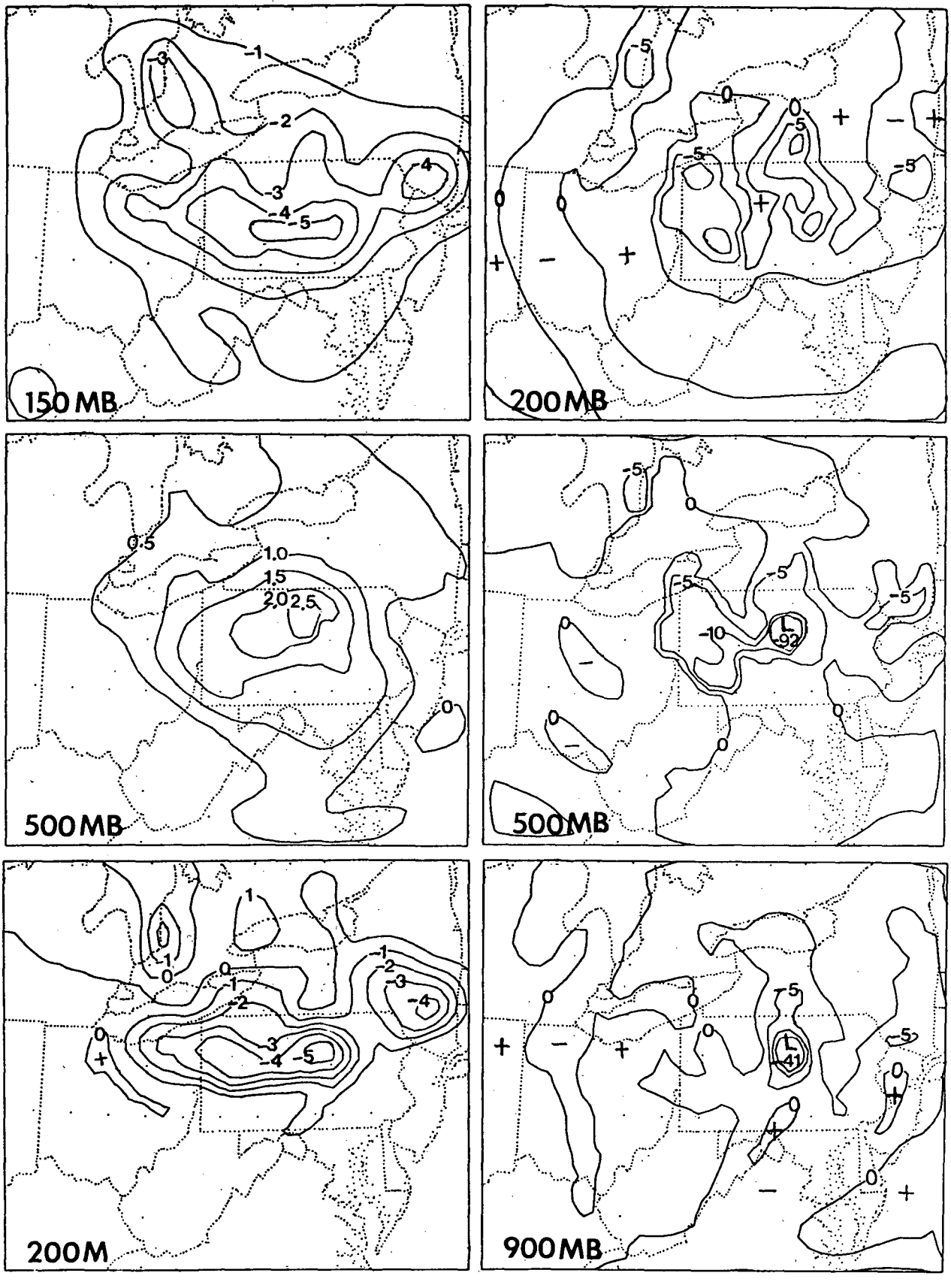

FIG. 5. Difference fields from 12 h into the simulation between the control simulation and Exp. NDH (no diabatic heating). The left panel is for temperature (°C) and the right for vertical motion (ω, μb s^{-1}).

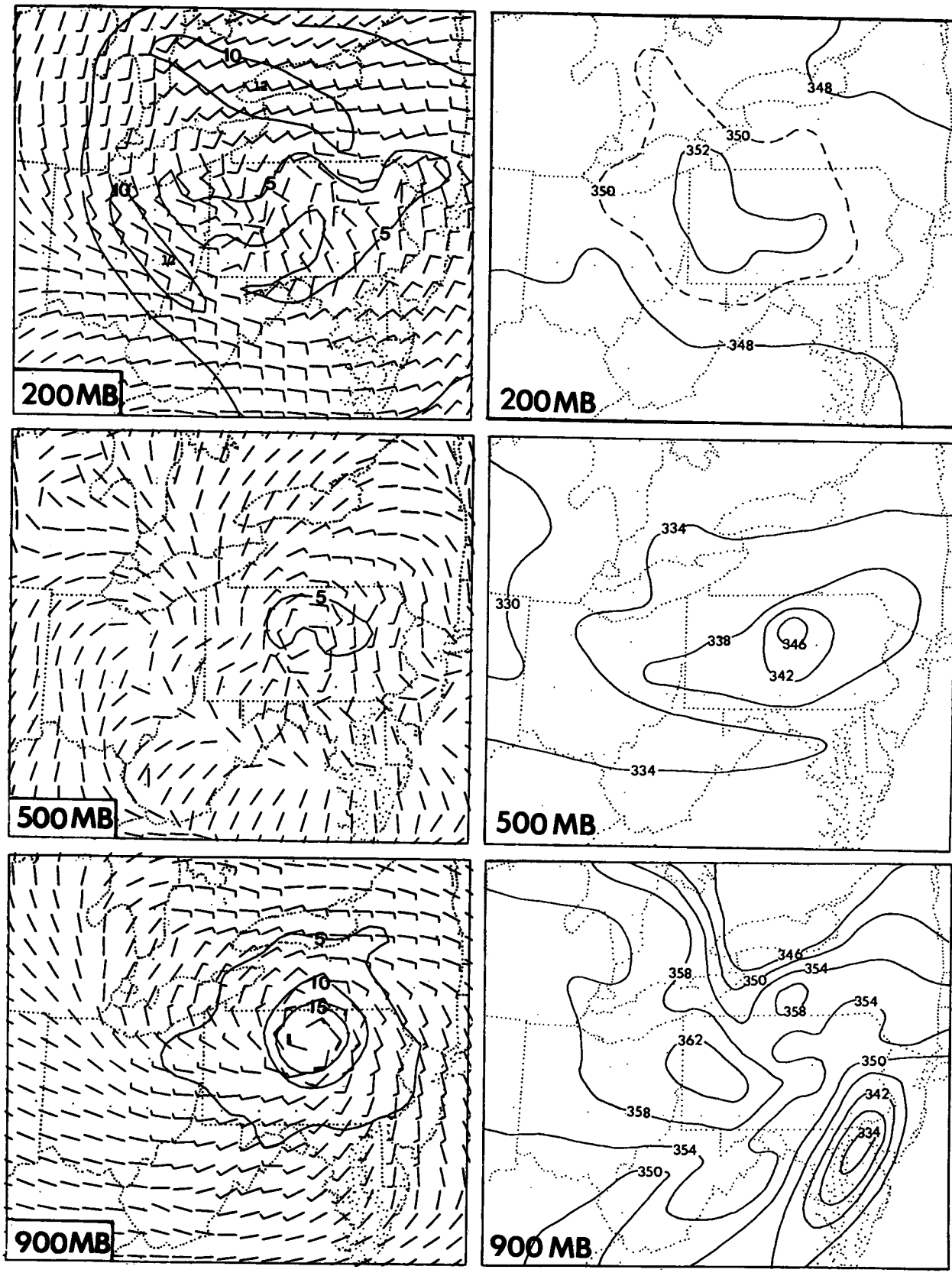

FIG. 6. Left panel is the same as Fig. 5 but for horizontal wind (m s^{-1}). The right panel is equivalent potential temperature from 12-h control simulation.

area of vertical motion is generated by the MCSs. The pattern is almost in phase vertically and the strongest upward motion is associated with the mesovortex. Note the low-level upward motion above the moist downdraft outflow boundary over eastern Ohio and western Pennsylvania (cf. Figs. 1 and 5). This is the region where both observed and modeled convection continued to develop during the evening hours. There is also upward motion over portions of southern Pennsylvania, Maryland and Virginia. This favorable condition, created by the MCSs, helps the deep convection advance into these regions later in the evening.

Along with the well-defined thermal and vertical motion perturbations, the MCSs also generated strong perturbations in the horizontal wind field (see Fig. 6). In particular, the perturbation wind vectors show a distinct cyclonic circulation from low- to midlevels and a well-defined anticyclonic circulation in the upper troposphere. When coupled with the equivalent potential temperature (θ_e) field (see the right panel of Fig. 6), it is evident that the low- and midlevel cyclonic circulation tends to bring low-θ_e air from the southeastern portion of the model domain into eastern Pennsylvania. This probably contributed to the temporary weakening of the squall line. At upper levels, the anticyclonic flow exports the high-θ_e air over a broad area surrounding the MCSs (ventilation effect). Note that the strongest cyclonic flow occurs near the center of the mesovortex (probably as a result of angular momentum conservation as air parcels approach the vortex). On the other hand, the strongest anticyclonic flow occurs hundreds of kilometers away from the mesovortex. The characteristic blocking effect of MCSs on the upper-level flow (see Fritsch and Maddox, 1981a; Maddox et al., 1981; Wetzel et al., 1983) is clearly apparent upstream (to the west) of the MCSs, while to the north, the westerly perturbation component (when coupled with the mean westerly flow) indicates the formation of an upper-level jet streak. The resulting anticyclonic outflow is an indication of an upper-level mesohigh produced by the MCSs.

The generation of significant perturbations in the wind and thermal fields by the Johnstown MCSs conforms to previous observational and numerical investigations (Ninomiya, 1971a,b; Fritsch and Maddox, 1981a,b; Chang et al., 1982; Perkey and Maddox, 1985). All of these studies suggest that latent heat release and sensible heat redistribution play an important role in the amplification and maintenance of the larger-scale systems within which MCSs are embedded. In particular, the effect of diabatic heating can become even more significant when an MCS occurs in a weak-gradient summertime environment. Thus, a model's skill in predicting the timing and location of the occurrence of MCSs may have a significant effect not only on the smaller-scale weather phenomena, but on forecasts of large-scale atmospheric structure, as well.

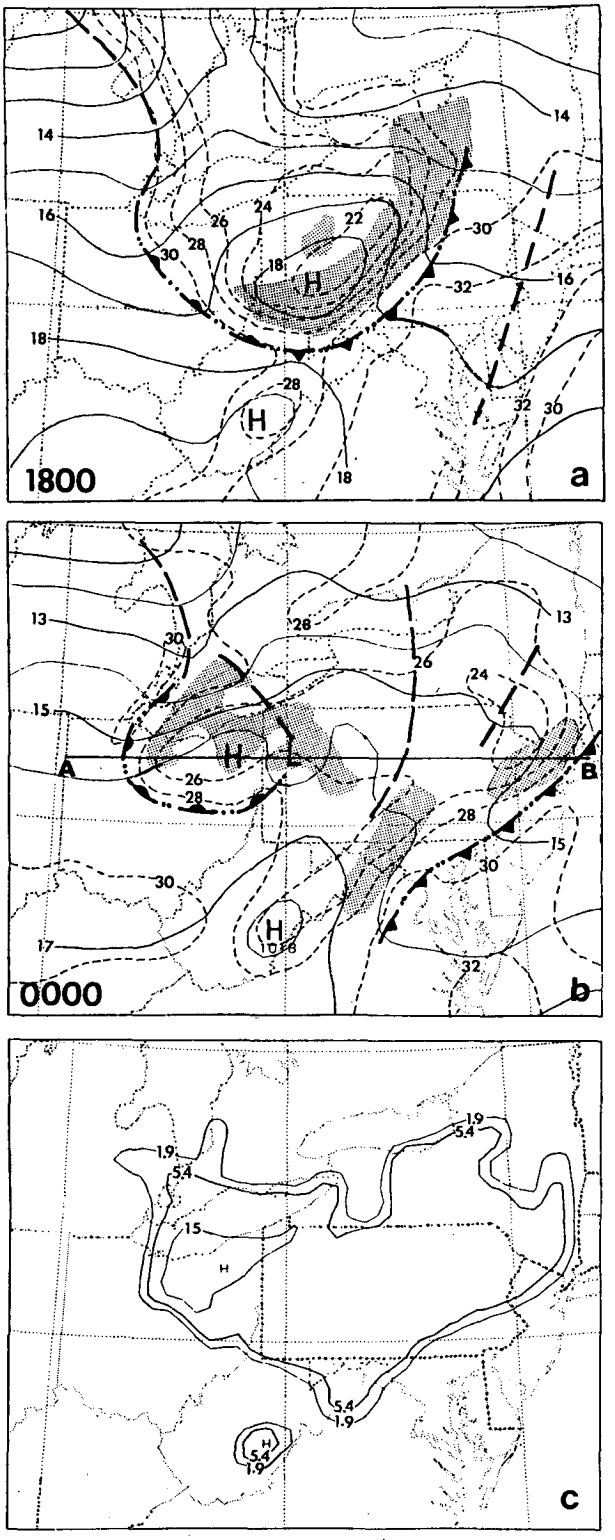

FIG. 7. (a–b) Predicted evolution of sea-level pressure (solid lines, mb), convective activity (shaded region), and surface temperature (dashed lines, °C) for Exp. CPS (convective effect). (c) Predicted 12-h accumulated rainfall (mm) for the period 1200 UTC 19 to 0000 UTC 20 July 1977.

b. Convective versus resolvable-scale heating

In this section, the results of two experiments are described. In the first experiment (CPS), only the heating produced by the FC convective parameterization is introduced into the model governing system of equations; resolvable-scale condensation heating is excluded. The second experiment (RSC) is the reverse of Exp. CPS, i.e., resolvable-scale condensation heating is permitted, but "convective" heating is excluded. Figure 7 summarizes the results of Exp. CPS. The most obvious difference between CPS and CTS (the control simulation) is that the major mesolow over northwestern Pennsylvania did not materialize (cf. Figs. 1 and 7). Correspondingly, neither did the very heavy rainfall. On the other hand, the squall line and the redevelopment of deep convection on the western flank of the moist downdraft outflow was reproduced. This suggests that the development of the mesolow/MCC is closely related to the resolvable-scale ("stratiform")[3] condensation. The notable contribution of stratiform precipitation has been documented by many studies to be a characteristic of MCCs (see Maddox, 1980, 1983; Rockwood et al., 1984; Leary and Rappaport, 1987; Smull and Houze, 1985) and tropical squall lines (see Houze, 1977; Leary and Houze, 1979a). To make sure that the relative roles of the parameterized versus resolvable-scale moist processes are not convective-scheme dependent, the Anthes/Kuo type of convective scheme was tested in the same way as Exp. CPS. The model again failed to generate the mesolow and associated rainfall (not shown). It appears that the reproduction of the mesolow requires a heating maximum at relatively low levels; this is discussed further later in this section.

Without the mesovortex, a stronger mesohigh and associated moist downdraft outflow developed with the squall line (cf. Figs. 1 and 7). Moreover, the strong southerly low-level flow of relatively low-θ_e over eastern Maryland, Delaware, eastern Pennsylvania and New Jersey did not develop (see Fig. 6). Consequently, the squall line advanced farther south and east in Exp. CPS than in the control run. These changes imply that successful prediction of the evolution of MCSs may hinge upon the interaction among many cloud-scale and mesoscale phenomena such as mesohighs, mesolows, deep convection, resolvable-scale condensation, moist downdrafts, etc.

The results of excluding the parameterized deep convection but allowing the feedback of resolvable-scale condensation heating (Exp. RSC) are shown in Figs. 8 and 9. The most obvious effect of leaving out the convection is the much more intense mesocyclogenesis and continued development of the mesolow in central Pennsylvania. Specifically, after 12 hours of in-

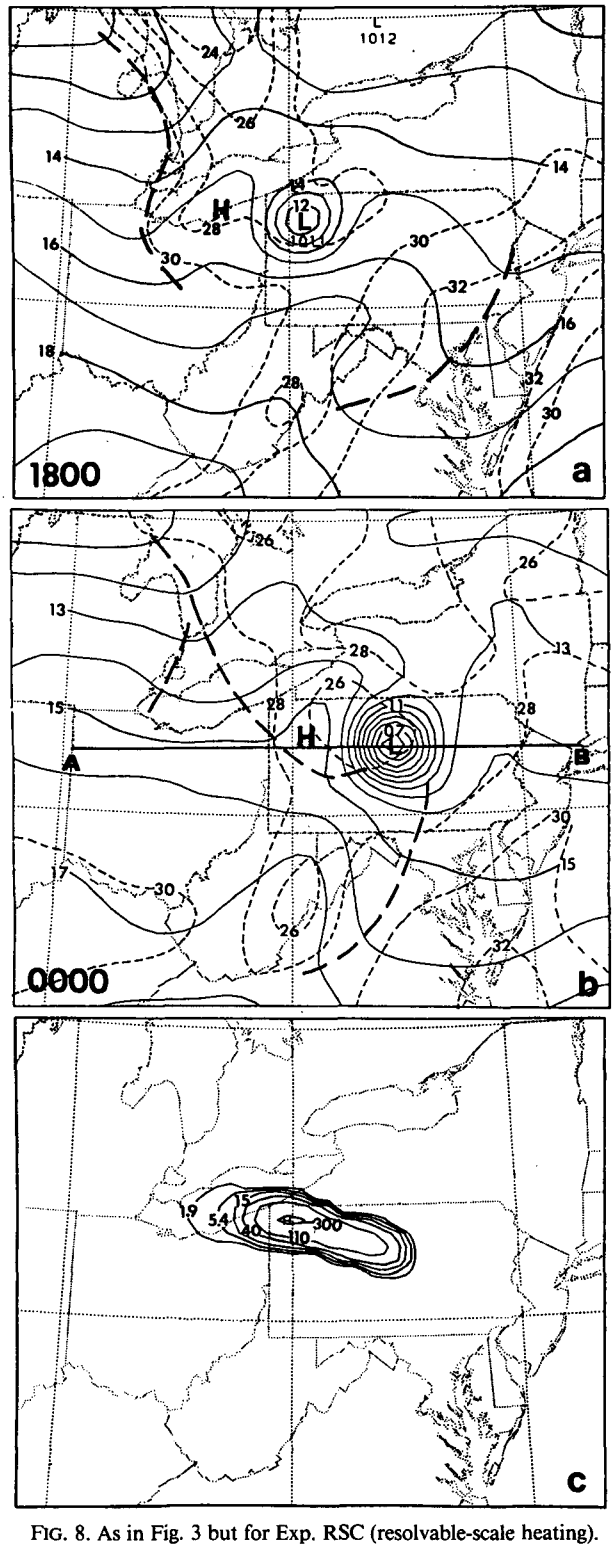

FIG. 8. As in Fig. 3 but for Exp. RSC (resolvable-scale heating).

[3] The term "stratiform" is used rather loosely here since Leary and Rappaport (1987) have shown that, at least in some instances, the so-called stratiform regions are actually marginally convective. A more appropriate term, from the viewpoint of numerical modeling, is "grid-resolvable scale" condensation.

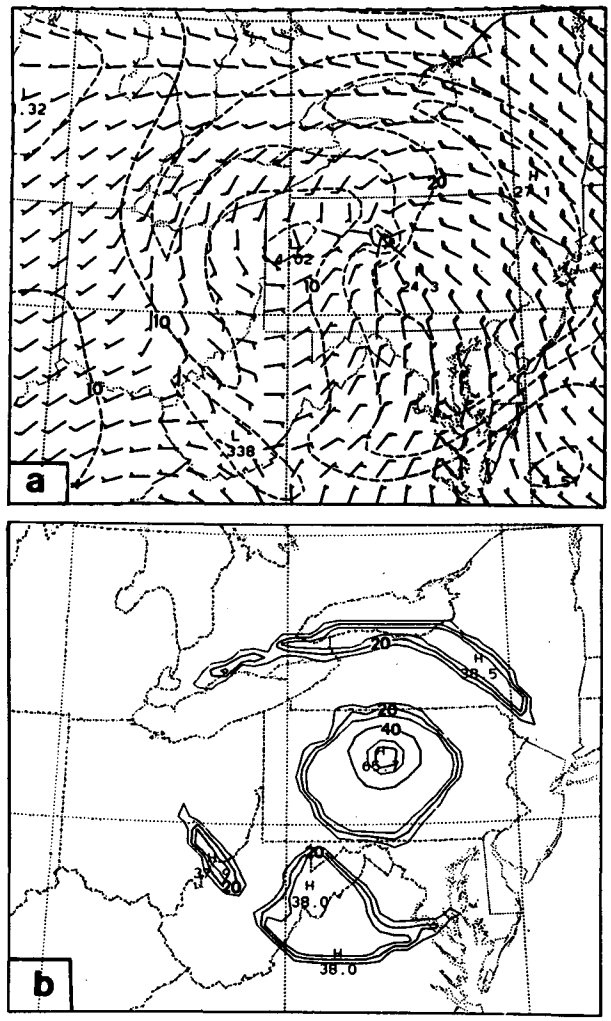

FIG. 9. (a) 12-h forecast of 200 mb winds (m s^{-1}) for Exp. RSC (resolvable-scale heating). (b) 12-h forecast upper-level cloud fraction for Exp. RSC. Cloud fraction (n) is defined by: $n = 3.2RH - 2.4$, where RH is the relative humidity. Partial cloud cover is assumed to start when RH reaches 0.75 (see Benjamin and Carlson, 1986).

tegration time, the minimum sea-level pressure and the maximum precipitation in Pennsylvania have respective magnitudes of 1005 mb and more than 300 mm, compared to the 1011 mb and 110 mm for the control simulation (cf. Figs. 1e, 1f and 8). Furthermore, the total precipitation exceeded the control case by almost a factor of two (see Table 2). The tendency for the resolvable-scale condensation to produce excessive rainfall can also be found in Molinari and Dudek (1986) and Kalb (1987). As found by Zhang and Fritsch (1986b), the positive feedback cycle among latent heating, low-level mass and moisture convergence, and surface pressure deepening resulted from the near-saturated and moist adiabatic stratification over Lake Erie in combination with the centralized upward lifting from the mesoα scale short wave at the model initial time. This type of a response is similar to the resolvable-scale gravitational or CISK-like instability discussed by Kasahara (1961) and Zhang et al. (1988). As a result of the intensifying mesolow, the lower- and upper-level flows exhibit strong cyclonic-convergent inflow and anticyclonic divergent outflow, respectively. Figure 9a shows the 12-h forecast wind at 200 mb for Exp. RSC. Note the band of strong wind downstream (northeast) and very weak wind upstream (west) of the mesovortex. There also appear to be internal gravity waves propagating radially outward from the center of the upper-level anticyclone. This is apparent in the distribution of the upper-level cloud fraction (see Fig. 9b) which clearly shows similarity to the distribution of cirrus bands visible above tropical cyclones.

In subsection 4a, it was shown that diabatic heating produced an amplification of the traveling mesoα-scale short wave (see Fig. 4b). Since a number of papers have hypothesized that deep convection may be responsible for the rapid deepening of extratropical cyclones (see Tracton, 1973; Gyakum, 1983), it is worthwhile to examine the relative contributions of convective versus resolvable-scale heating to the deepening of the mesoα-scale wave. Figure 10 compares the control run 700 mb height field valid at 0000 UTC to the forecast fields that result when 1) all latent heat release is excluded, 2) only heating from deep convection is permitted, and 3) only resolvable-scale latent heat release is allowed. The 700 mb level was selected for comparison since this is the approximate level where the maximum wave amplification was observed to occur (see Hoxit et al., 1978, and Figs. 10e and 10f). Although it is clear from Fig. 10 that the convective heating contributes to the deepening of the short wave, resolvable-scale heating seems to have the greatest impact. Moreover, it was shown in Zhang and Fritsch (1987) that the effects of the resolvable-scale heating develop very quickly and are directly responsible for the rapid spinup of the warm-core vortex.

The faster and greater impact of resolvable-scale heating relative to convective cloud heating probably stems from differences in the vertical distribution of heating between the two modes of condensate production. These differences can be seen with the aid of Figs. 11 and 12. Specifically, it is apparent from Fig. 11 that the resolvable-scale heating exhibits a maximum in the midtroposphere rather than the high-level maximum from the deep convection. Heating profiles with a high-level maximum tend to cause more *middle* tropospheric mass and moisture convergence than those with low- to midlevel maxima (see Fritsch, 1986). Because midlevel air is often relatively cool and dry during the onset of convective episodes, a long period of time is usually required to adjust the environment towards a more moist adiabatic profile. Convectively forced midlevel convergence and ascent, coupled with moisture detrainment from convective clouds, tends to produce such an adjustment, i.e., toward a relatively warm, nearly saturated mesoscale region with a lapse rate close

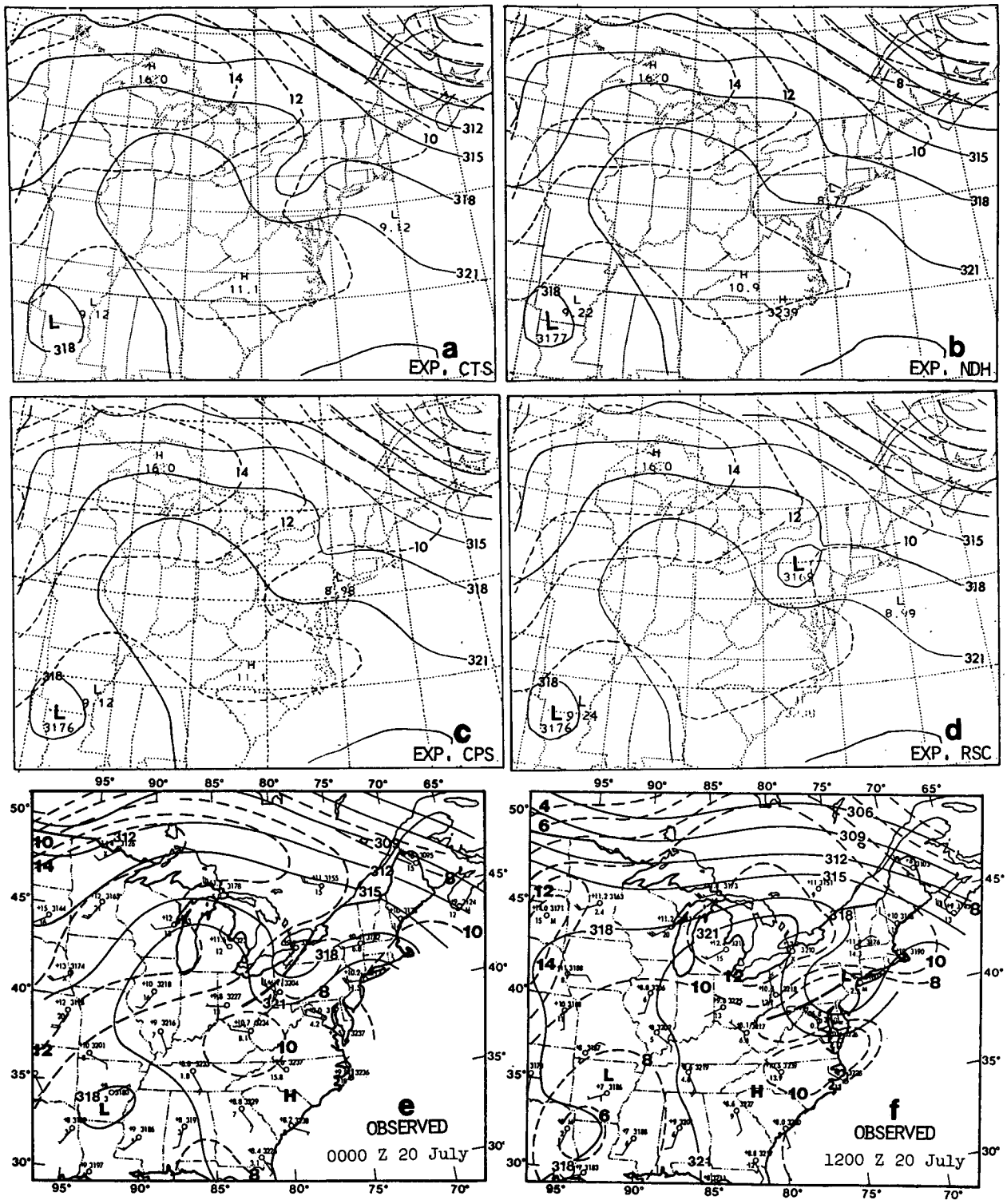

FIG. 10. Comparison of 700 mb heights (dam) and temperature (°C) at 0000 UTC 20 July for (a) Exp. CTS (control simulation); (b) Exp. NDH (no diabatic heating); (c) Exp. CPS (convective effect); (d) Exp. RSC (resolvable-scale heating); and observed conditions at (e) 0000 UTC 20 July and (f) 1200 UTC 20 July.

to the moist adiabatic. With continued vertical motion this region would be characterized by high-based "stratiform" clouds. In the Johnstown case, this process had occurred intermittently for several days prior to the vortex development (see Bosart and Sanders, 1981). Thus, the mesoscale environment in which the vortex

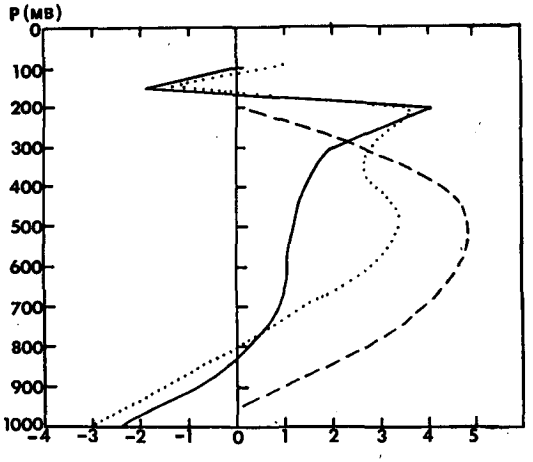

FIG. 11. Typical profiles of parameterized convective heating (solid line; °C h^{-1}), resolvable scale heating (dashed line; °C h^{-1}), and 12-h composited heating (dotted; °C per 12 h) for the present case study.

developed was nearly saturated and exhibited a neutral to slightly conditionally unstable lapse rate (see Zhang and Fritsch, 1986b). Figure 12a shows that under these conditions, and without the presence of deep convection, pronounced *midlevel* warming was produced by the resolvable-scale condensation. On the other hand, when only the effects of deep convection are introduced, midlevel temperature changes (in a drier region with a steeper lapse rate) are relatively small. Note though that significant warming occurs in the upper troposphere and moist downdrafts produce substantial cooling in the lowest 100 mb. Note also that resolvable-scale condensation eventually developed over northeastern and western Pennsylvania where convection persisted in the model simulation (see Zhang and Fritsch, 1987). A similar development of resolvable-scale condensation in response to convective forcing also occurred in simulations by Kreitzberg and Perkey (1977) and Perkey and Maddox (1985).

These results suggest that resolvable-scale condensation made a substantial contribution to the shortwave amplification in the present case. They also suggest that the explosive deepening of extratropical cyclones such as documented by Sanders and Gyakum (1980) may not be directly a result of deep convection, as hypothesized. On the other hand, it must be stressed that it is the deep convection that is instrumental in modifying the environment in such a way as to create the favorable dynamic and thermodynamic conditions that cause or allow the resolvable-scale condensation to materialize (see Zhang and Fritsch, 1987 for additional discussion). Moreover, it is important to point out that there is little delay in the start of resolvable-scale condensation with the present grid resolution. With a 1° latitude–longitude mesh for the same case and sensitivity test as Exp. RSC, Molinari and Corsetti (1985) reported 96% underestimations of 12-h total rainfall due to the significant delay in resolvable-scale heating.

Finally, it is extremely important to note that the time- and space-composited heating profile for the 12-h episode (1200 UTC 19 July–0000 UTC 20 July) is very similar to profiles diagnosed for other MCSs (cf. the profile shown in Fig. 11 and those obtained by Ninomiya, 1971a; Lewis, 1975; Johnson, 1976). This is an interesting result since, based on the model results, it is clear that the composite profile is composed of both convective *and* resolvable-scale processes. Therefore, as noted by Johnson (1984), it may be inappropriate to refer to heating profiles diagnosed using conventional sounding data as "convective" and expect a convective cloud model in a convective parameterization routine to generate such a profile. Moreover, any

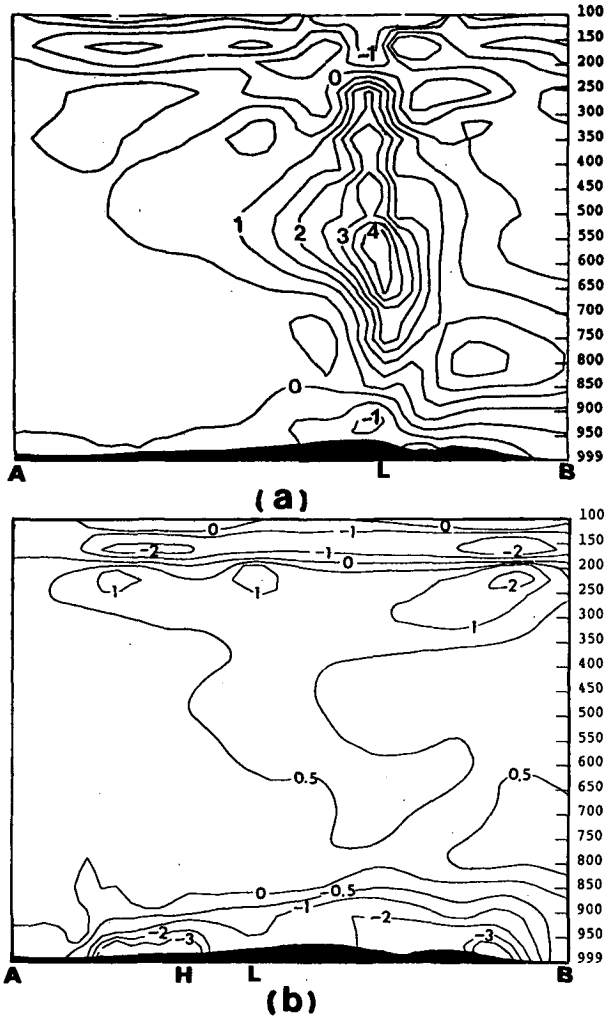

FIG. 12. Cross-sectional comparison of 12-h forecasted differences in troposphere temperature (a) between Exps. RSC (resolvable-scale heating) and NDH (no diabatic heating) (see Fig. 8b for the location); and (b) between Exps. CPS (convective effect) and NDH (see Fig. 7b for the location).

attempts to "tune" a convective cloud model so that it will produce such a profile may introduce serious errors into the formulations for such processes as cloud entrainment/detrainment, precipitation efficiency, water loading, etc. Most importantly, if the *composite* profile from Fig. 11, or a similar profile obtained diagnostically, is used in convective parameterization in a fine-grid mesh model, it is clear that there is a substantial risk that the model will catastrophically fail in its attempt to reproduce or predict the structure and evolution of MCSs.

A significant caveat to the model results and to the preceding discussion is that the model simulations did not include precipitation drag, melting and subcloud-layer evaporational cooling of resolvable-scale precipitation. As shown by Zipser (1977), Leary and Houze (1979b), Brown (1979), Leary (1980), Molinari and Dudek (1986), Zhang et al. (1988) and others, these processes tend to produce mesoscale downdrafts and vertical stabilization in the lowest 200–400 mb of the atmosphere. In view of the sensitivity of the mesovortex to the *cloud-scale* downdrafts, it is likely that if these resolvable-scale processes were included in the model, they would introduce an additional drag on the development of the mesovortex, i.e., the resolvable-scale circulation could not as easily "access" high θ_e air. In this particular case (i.e., the Johnstown flood event), weakening of the mesovortex in the lowest model layers is a desirable effect since the model appeared to overpredict the vortex in the control simulation (see Zhang and Fritsch, 1986a, and the subsequent discussion).

c. *Effect of parameterized moist downdrafts*

By turning off the downdraft effect in the FC convective scheme (Exp. NPD) the squall line propagated more slowly and exhibited a significantly weaker pressure perturbation than that in the control run (cf. Figs. 1 and 13). In particular, after 1800 UTC, the squall line gradually lost its southwest–northeast line structure and failed to move into eastern Pennsylvania. The failure of the squall line to move into this region can also be seen in the 12-h accumulated rainfall distribution (see Fig. 13d). Moreover, the model MCC shows no evidence of southerly propagation of convective activity into southern Pennsylvania, Maryland or Virginia during the model evening hours. Correspondingly, without the moist downdrafts, the boundary layer temperatures associated with the deep convection are much too warm in comparison with the observed or control-run temperatures, and therefore the static stability is much less. In fact, because of neglecting the stabilizing effects of the downdrafts, the mesolow that developed mainly as a result of *resolvable-scale* condensation was strongly overpredicted. Specifically, after *18 hours* of integration time, the minimum sea-level pressure of the mesolow and accumulated precipitation volume have respective magnitudes of 1004 mb and 8.48×10^{12} kg, compared to 1012 mb and 5.33×10^{12} kg for the control simulation (not shown). Other noticeable changes are that the model erroneously maintained the quasi-stationary convective activity along the Ohio–Lake Erie boundary and in southern New York, failed to generate the mesohigh over northeastern Pennsylvania, and produced a much weaker pressure perturbation over western Pennsylvania.

When the updraft effects were excluded but the downdraft effects were retained in the FC scheme (Exp. NPU), the squall line became discontinuous and moved slightly faster than in the control case (see Fig. 14). Moreover, the resulting surface pressure perturbations were significantly weaker. The most interesting difference, however, is that the absence of convective updrafts inhibits the development of the "resolvable-scale" mesolow and associated heavy precipitation. A final difference worth noting is that, unlike the Exp. NPD, the model convection gradually diminished after 0000 UTC and was gone by 0600 UTC (not shown). However, it is important to recognize that just the downdrafts, coupled with the forcing from the mesoα-scale short wave, were capable of initiating and organizing deep convection for over 12 hours.

It appears that the downdrafts behave in one sense as a "brake" on the energy supply for the Johnstown MCSs by incorporating lower-θ_e air into the PBL (e.g., the weakening of the mesolow and shorter duration of convection over northern Ohio and New York in the control simulation), and in another sense as a generator of convection through enhancement of low-level convergence (e.g., the progressive squall line, widespread and continued convection over western Pennsylvania, southerly propagation of convection into Maryland and Virginia during the evening hours in the control case). The "brake" effect can be understood as a *vertical* process in which the low-level cooling and drying not only tend to stabilize the atmospheric column and suppress the occurrence of deep convection, but to remove moisture that otherwise would be used for stratiform condensation (e.g., no mesolow in Exp. NPU, and a stronger mesolow in Exp. NPD). A similar conclusion has been reached by Molinari and Corsetti (1985), i.e., the incorporation of downdraft effects into the Kuo-1974 cumulus parameterization scheme significantly increased the rate of resolvable-scale stabilization and produced a better forecast of the 12-h accumulated rainfall volume. On the other hand, the downdraft air within the subcloud layer, in association with upper-level convective heating, can enhance the *horizontal* pressure gradient across the cold outflow boundary such that strong convergence occurs. In addition, because of the large horizontal temperature gradient across the boundary (see Fig. 5), the thermal wind (vertical wind shear) may be altered and in certain circumstances a low-level jet may result (see Maddox et al., 1980). The combination of these two opposite effects is clearly noticeable during the evening hours when the

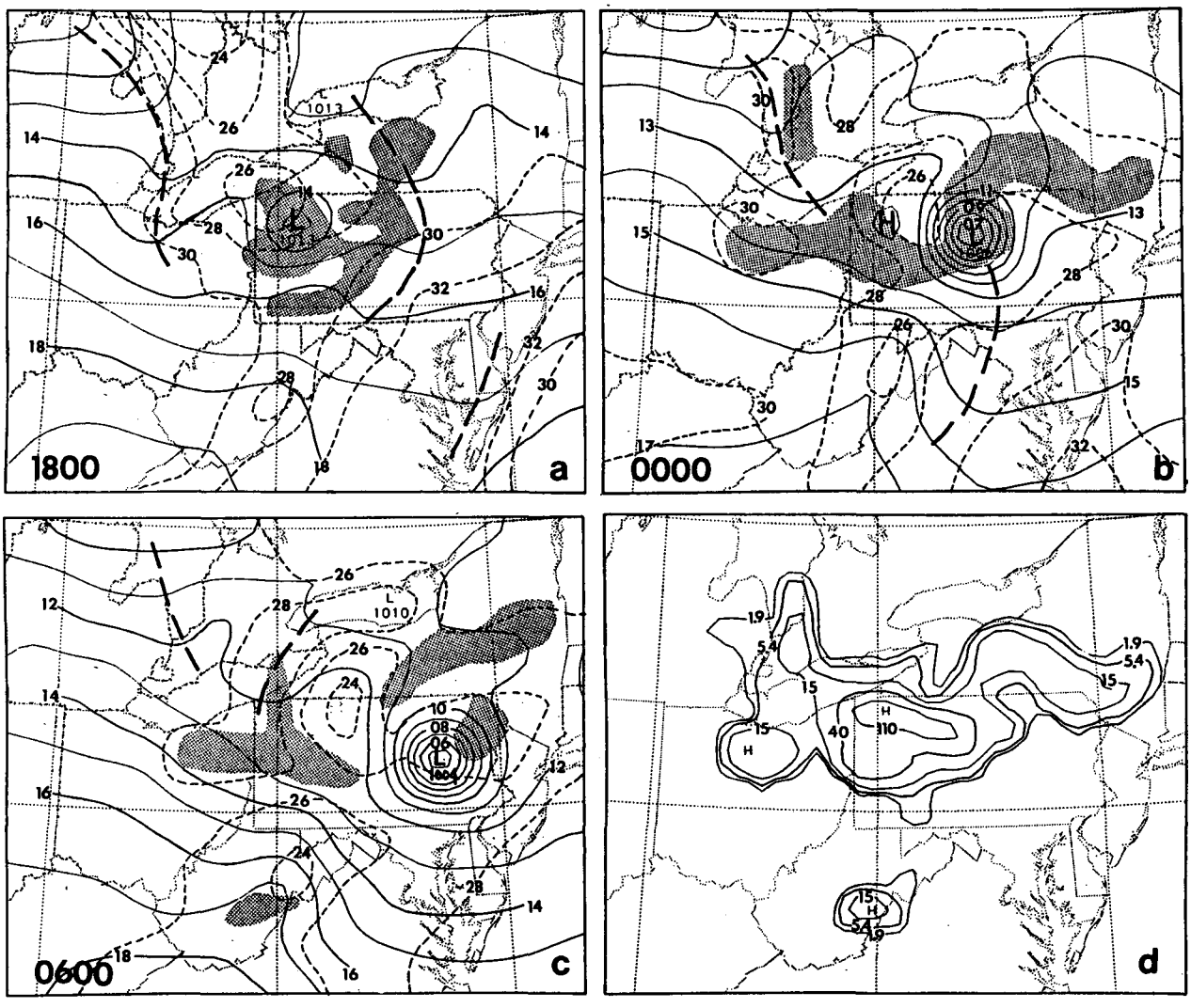

FIG. 13. As in Fig. 7 but for Exp. NPD (no parameterized downdrafts) and the 18-h results are shown.

boundary layer was still warm and the cumulative cooling from previous convection formed a well-defined thermal boundary along western Pennsylvania, Maryland, Delaware and southern New Jersey. In particular, as the low-level jet continuously transported moist static energy into the MCC region, the cold outflow over western Pennsylvania acted as a quasi-stationary warm front in which the higher-θ_e air overran the downdraft air (see Zhang and Fritsch, 1986a, 1987).

d. Performance by the AK scheme

Figure 15 shows the evolution of surface features using the AK type of convective parameterization scheme. Note that the shading in Fig. 15 indicates the areas where convection occurred in any of the ten model time steps (6 min) prior to the indicated time of each panel in the figure. This 6 minute compositing of convective activity is used to show the location of convection because the convective effects computed by the AK scheme are based upon instantaneous values of moisture convergence, and this sometimes (as observed in this study) appears to be influenced by fast propagating Lamb waves. It is encouraging to note that the AK scheme is capable of generating some mesoβ-scale features. In particular, the sqall line and the separation of the squall line from the pre-MCC seem to be captured by the simulation. Note though, that a coarser-mesh (0.5° latitude–longitude) application of a Kuo-type scheme to the Johnstown event was unable to generate these features (see Molinari and Dudek, 1986) even though the initial conditions were similar. This suggests that high resolution may be necessary for the numerical simulation of the detailed mesoscale structure and evolution of the Johnstown flood and possibly other MCS events.

Although the AK scheme simulated the separation

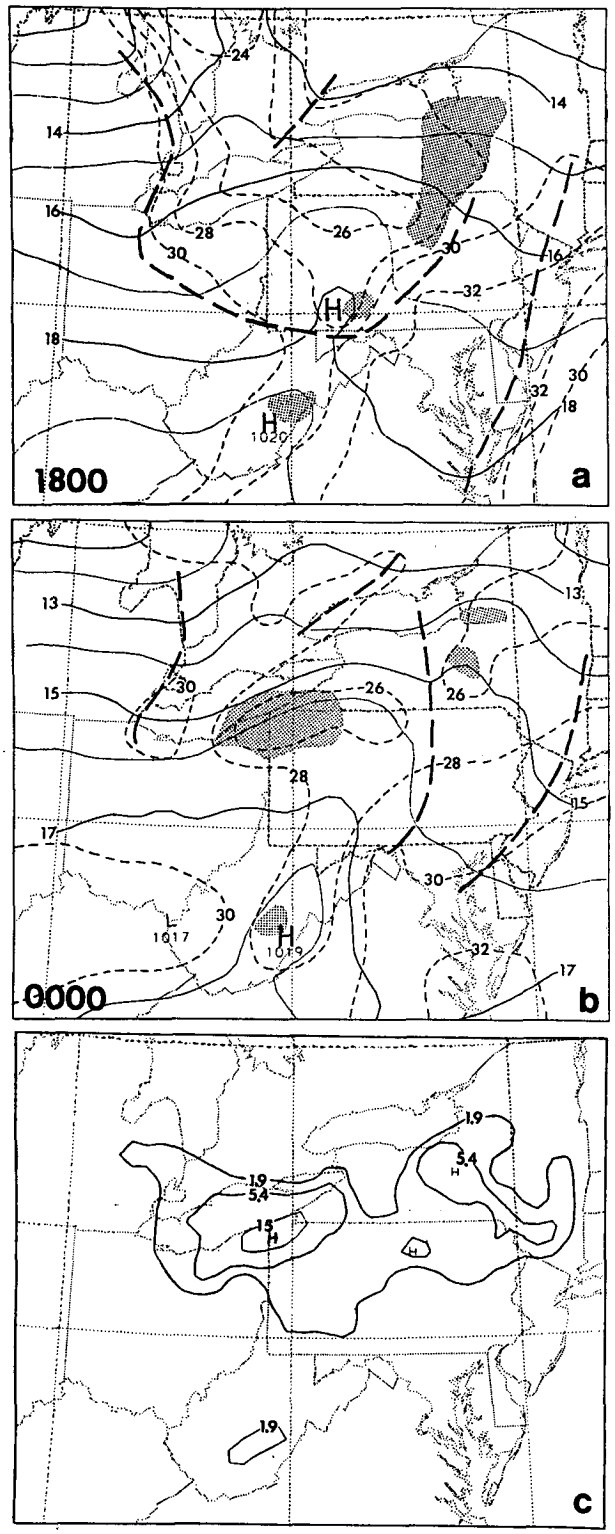

FIG. 14. As in Fig. 7 but for Exp. NPU (no parameterized updrafts).

of the squall line from the pre-MCC, it occurred too soon and the squall line dropped insufficient precipitation (≤2 mm) as it propagated into eastern Pennsylvania. The 12-h accumulated *convective* rainfall volume is only 40% of the rainfall total and 45% of the control-predicted convective rainfall. The premature separation of the convective systems may possibly be the result of the dependence of convective activity on the moisture convergence since as the mesovortex develops, the mesoscale compensating subsidence in the region immediately adjacent to the vortex (see Fig. 5) tends to reduce the amount of moisture convergence. The insignificant rainfall associated with the squall line is probably related to insufficient moisture convergence over eastern Pennsylvania and the surrounding region. This in turn is probably a result of two factors: 1) the lack of cold downdrafts in the AK scheme and 2) a relatively small mass perturbation induced by the convective heating. The latter can be attributed to the computed large values of the "b" parameter in this case (see Kuo, 1974 for definitions). For the simulated squall line, the "b" value is larger than 0.4 while the FC-scheme-generated value is about 0.1–0.2. Fritsch et al. (1976) and Ogura and Jiang (1985) found that the "b" parameter for midlatitude convectively driven systems can take large negative values since the deep convection under such circumstances tends to respond more to the magnitude of the local preexisting potential buoyant energy than to the larger-scale moisture convergence. Krishnamurti (1985) found a significant underestimation of convective heating when using a Kuo-type parameterization for initiating a monsoon circulation. Interestingly, he noted that when the "b" parameter was equal to zero, he obtained superior results. Moreover, Anthes (1985) commented that the Kuo type of convective parameterization may be inappropriate when it is used to simulate MCSs at the mature stage. In fact, budget studies (Ogura and Cho, 1973; Gray, 1973; Fritsch et al., 1976; Kuo and Anthes, 1984a) indicate that large-scale rates of mass and moisture convergence are insufficient to support some mesoscale convective systems.

In spite of the omission of moist downdrafts in the AK scheme, the mesohighs over eastern and western Pennsylvania and New York are well defined (see Fig. 15e). The fact that the mesohighs developed without moist downdrafts in the parameterization indicates that they may be dynamically produced. On the other hand, the size and location of the high-pressure systems may be simply a consequence of the development of the mesoβ-scale low pressure system in the middle of the traveling mesoα-scale surface ridge. This can easily be visualized by examining Fig. 3b (the simulation without diabatic heating) and imagining what the pressure pattern would look like if pressures over northcentral Pennsylvania were about 2 mb lower. The result would be mesoβ-scale ridges just to the east and west of central Pennsylvania. Apparently this same "superposition" phenomenon occurred in Exp. RSC ("convective" heating was excluded; see Fig. 8). Thus, it appears that moist downdrafts are not essential for development of

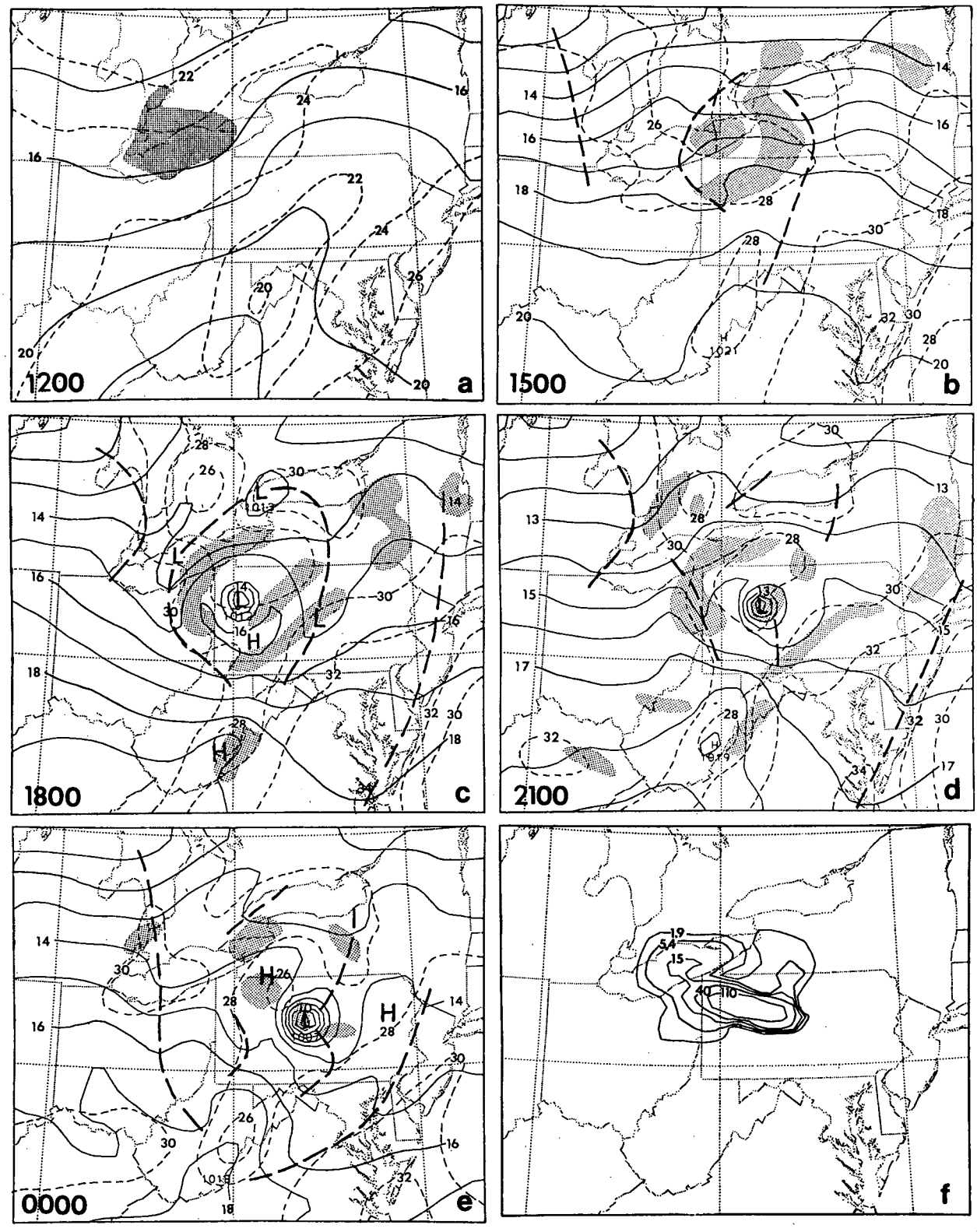

FIG. 15. As in Fig. 7 but for Exp. AKC (Anthes/Kuo scheme).

surface mesohighs associated with MCSs. However, it is important to note that the mesohighs were significantly stronger when moist downdrafts were included in the control simulation and in Exp. CPS (cf. Figs. 1, 7 and 15). Furthermore, the strong thermal gradients produced by the downdrafts apparently create vertical circulations that initiate and maintain deep convection while the "superposition mechanism" of mesohigh production does not. For example, the simulation with the AK scheme failed to reproduce the widespread convection associated with the MCC, and at the end of the 12-h integration, no important area of model convection was occurring over western Pennsylvania where it was both observed and simulated in the control run.

e. *Effect of boundary layer processes*

Without surface heating (Exp. NSH), the initial convective activity over Lake Erie gradually diminished as it propagated into northwestern Pennsylvania and the squall line did not develop (see Fig. 16). Apparently the failure to reproduce the squall line is due to the reduction in the potential buoyant energy and the ease with which the potential buoyant energy can be tapped. That is, as the boundary layer warms and the lapse rate increases, air parcels are much more likely to be buoyant when they arrive at their lifting condensation level (LCL) than when heating is absent. This is crucial for obtaining convective clouds in the FC parameterization scheme since, starting with the lowest model layer, successive layers are mixed, lifted and checked for buoyancy at their respective lifting condensation levels.

While the omission of surface heating grossly affected the convection, it did not affect the development of the mesolow nearly as much. This is probably because the mesolow forms primarily in response to the resolvable-scale vertical motion and latent heating and these are not *directly* affected by the surface heat flux. Note that the propagation and strength of the mesolow, as well as resolvable-scale precipitation (see Table 2), are comparable to that in the control simulation. Most of the rainfall (see Fig. 16c) is related to resolvable-scale processes; convective rainfall is less than 30% of the total amount. The convective activity over northwestern Pennsylvania (Fig. 16b) apparently is a result of lifting associated with the low-level jet, the temperature contrast between land and water surface, and the short-wave forcing in that region. The results of this experiment are especially interesting since in all the other sensitivity experiments where the deep convection and, in particular, the moist downdrafts are weaker than in the control run, the mesolow became significantly stronger. In this case it did not. The obvious implication is that the omission of surface heat fluxes has approximately the same stabilizing effect on the development of the mesolow as does the cooling by moist downdrafts. In this regard, note that the control-run moist downdraft temperatures in the middle of the day are about the same as the temperatures in the early morning and throughout Exp. NSH (cf. Figs. 1 and

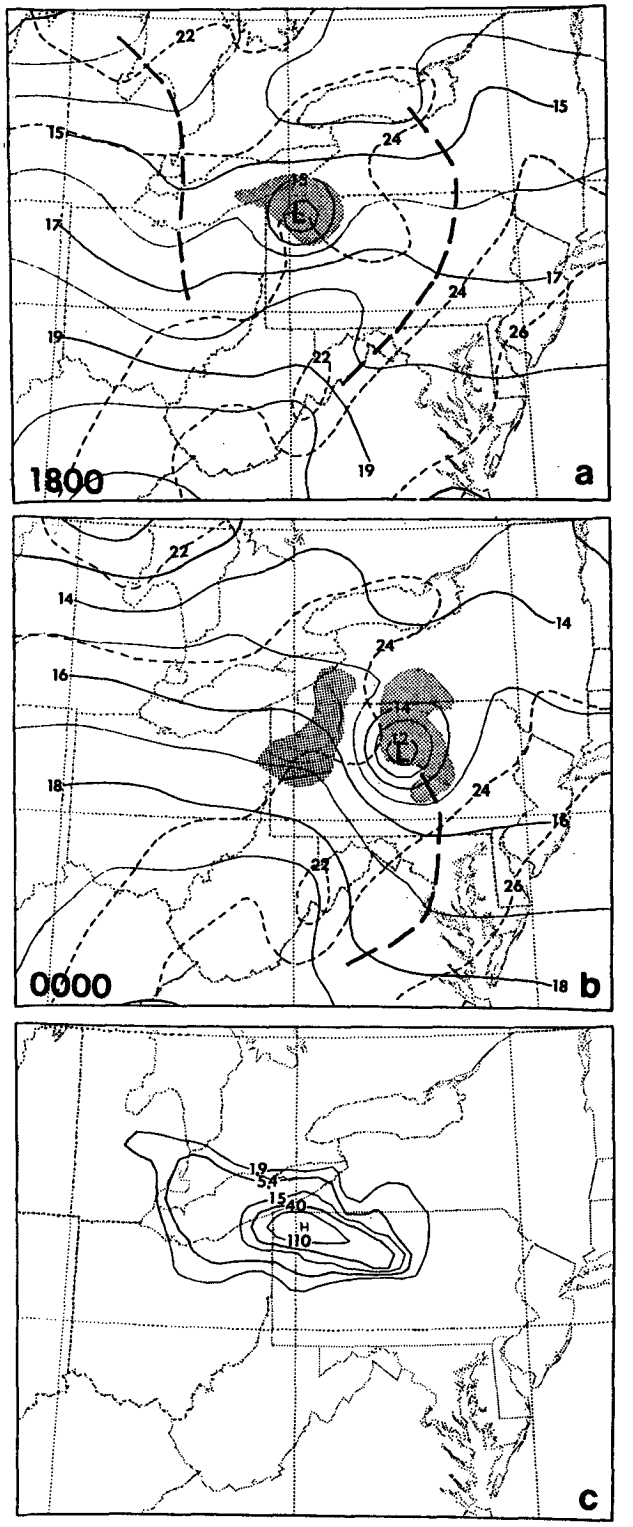

FIG. 16. As in Fig. 7 but for Exp. NSH (no surface heating).

16). The results of this experiment indicate that fine-mesh numerical models which include a diurnal heating cycle are susceptible to spurious overdevelopments of mesoscale pressure systems unless some type of stabilization process such as subcloud-layer evaporation (see Molinari and Dudek, 1986) or convective parameterization with moist downdrafts is introduced. Alternatively, without a diurnal heating cycle, significant mesolow developments and rainfall events may be missed.

When the bulk PBL formulation was used (Exp. BPL), the squall line propagated more slowly and exhibited weaker upward motion (not shown) and pressure perturbations than in the control simulation (cf. Figs. 1 and 17). Specifically, the squall line diminished very quickly after 1800 UTC and failed to move into eastern Pennsylvania (see Figs. 17b and 17c). Consequently, the mesohigh that was observed to form over northeastern Pennsylvania did not develop as it did in the control run. More importantly though, the weaker convection removed less of the low- to midlevel static energy and therefore the major mesolow was approximately 3 mb deeper than in the control run. Moreover, the mesohigh behind the low was weaker than in the control case. The results of this experiment reenforce the conclusions in the preceding paragraph and in Zhang and Fritsch (1987), i.e., the interaction between deep convection and other diabatic processes is crucial to successful simulation of MCSs.

For a dry PBL simulation, Anthes et al. (1980) compared the results of using a mixed-layer versus a multilevel model. They noted that under homogeneous terrain conditions, the mixed-layer model results agreed closely with that created by the multilevel model, while under complex terrain conditions, they did not. Apparently, under horizontally inhomogeneous conditions, the mixed-layer model is unable to represent the pressure gradient force that affects the prediction of the boundary layer flow in lower levels. The present results support their findings as shown by the sea-level pressure differences in Figs. 1 and 17. Moreover, Fig. 18 shows the terrain distribution used for this study and the 6-h forecasted 900 mb difference field of equivalent potential temperature (θ_e) between Exps. BPL and CTS. Note that the most significant differences clearly reflect the terrain orientation and terrain-related features (e.g., mountain waves, see Zhang, 1985). It appears that the bulk PBL formulation tends to overestimate the equivalent potential temperature on the upslope side of the terrain and underestimate it on the downslope side. This is probably part of the reason why the squall line did not propagate into eastern Pennsylvania when the bulk PBL formulation was used (see Fig. 17). These results suggest that the simple one-layer PBL formulation may be inadequate to represent the vertical fluxes of heat, moisture and momentum over mountainous regions with fine-resolution models. Compared to the bulk PBL version, Keyser and Anthes (1982) also found considerable improvement of the PBL structure using a version of the Blackadar scheme that is similar to the version used in the present study. In another study,

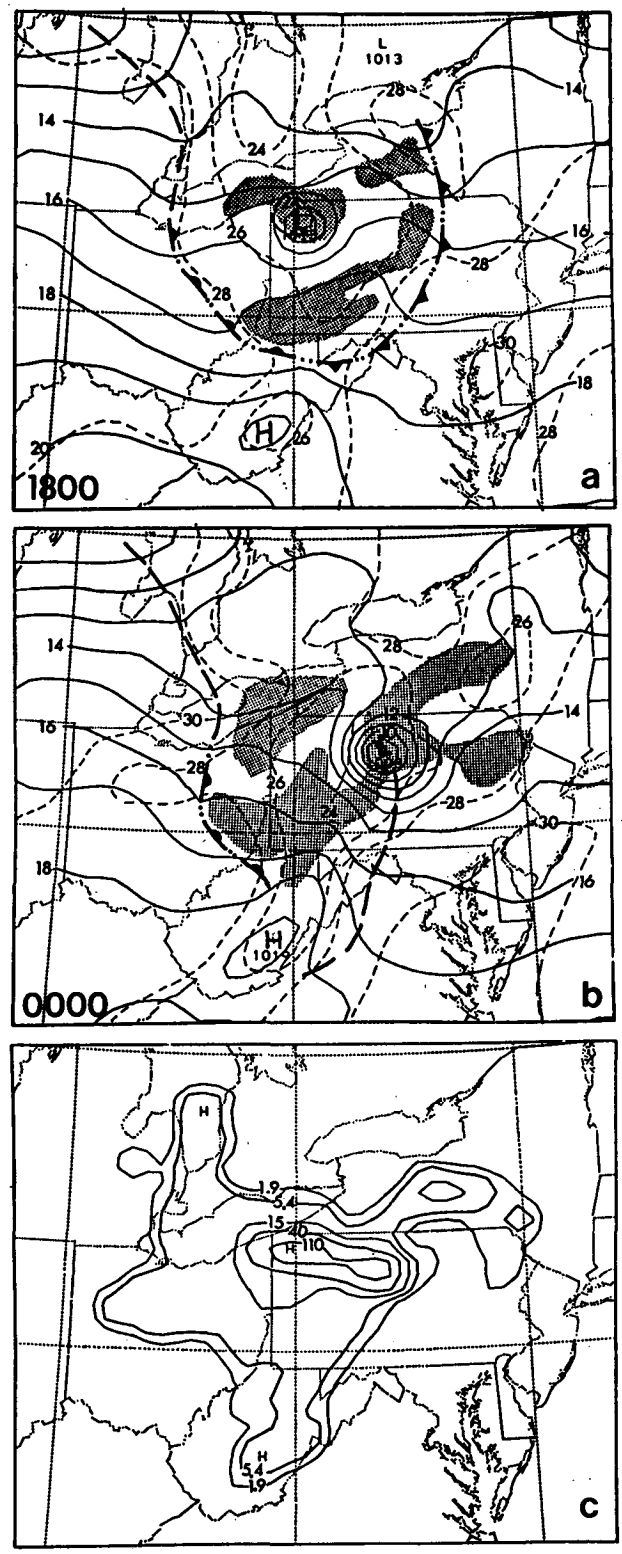

FIG. 17. As in Fig. 7 but for Exp. BPL (bulk PBL).

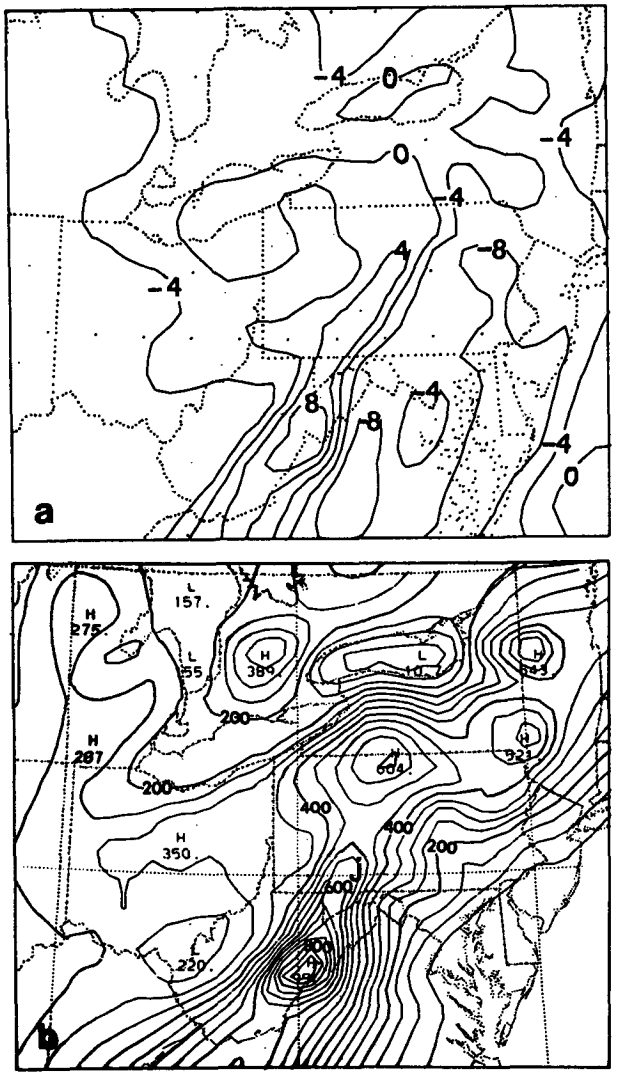

FIG. 18. (a) Difference fields (K) of 900 mb equivalent potential temperature between Exps. BPL (bulk PBL) and CTS (control simulation) for the 6-h forecast verifying at 1800 UTC 19 July 1977; (b) fine-mesh terrain distribution used for this study.

Bosart (1981) noted that the bulk PBL used in the LFM was responsible for part of the error in the QPF and sea-level pressure pattern for the Presidents' Day storm (18–19 February 1979). In the case of the Johnstown MCSs, accurate treatment of surface and PBL fluxes, and explicit resolution of the vertical variation of thermal and wind fields are essential for a successful simulation. The results also suggest that a multilevel PBL formulation may be necessary to predict other terrain-related convective systems, such as the MCSs that frequently initiate along the eastern slopes of the Rocky Mountains (see Wetzel et al., 1983; Cotton et al., 1983). In general, one would expect that a better representation of the diurnal cycle would tend to improve prediction of convective precipitation in fine-resolution models since the generation of local θ_e maxima would also be improved and therefore the prediction of the timing, frequency, and location of convective cloud development would be enhanced.

f. Effect of virtual temperature

As mentioned before, the inclusion of virtual temperature instead of just temperature in the governing system of equations has two important effects: parcel buoyancy is increased and horizontal pressure gradients are altered. Using just temperature throughout the entire governing system of equations (Exp. VTP) produces a model result similar in many respects to Exp. CPS. Specifically, the model only reproduced the life cycle of the squall line but missed all of the mesolow/MCC and its associated convective activity (see Fig. 19).

The effect of virtual temperature on buoyancy has been recognized in many studies using cloud models (e.g., Lopez, 1973; Anthes, 1977; Kreitzberg and Perkey, 1976). However, its effect on the horizontal pressure gradient and the corresponding wind field is frequently ignored in simulations of large-scale features, particularly for wintertime events. During the spring and summer, however, moisture gradients can be extreme and, under weak flow conditions, may have a considerable effect on the height and wind fields. This effect can be quantitatively estimated through the computation of the thermal wind (V_T). Consider

$$V_T = \frac{R}{f} \ln \frac{P_2}{P_1} \nabla_p \bar{T}_v$$

$$= \frac{R}{f} \ln \frac{P_2}{P_1} [\nabla_p \bar{T} + 0.608(q\nabla_p \bar{T} + \bar{T}\nabla_p \bar{q})]. \quad (3)$$

(A) (B) (C)

Clearly, term B will always be much less than A and therefore can be neglected. If terms A and C are evaluated using the 0000 UTC 20 July values of temperature and moisture in the 600–700 mb layer between Flint, Michigan and Pittsburgh (the region of initial convective activity), then term A contributes about 6 m s^{-1} to V_T and term C offsets this by about half (i.e., -3 m s^{-1}). Considering that the observed wind speeds were only about 5 to 10 m s^{-1} in this region, it is evident that *the effect of moisture could have accounted for 25–50% of the geostrophic wind!* Since the mesovortex did not develop when virtual temperature was not included in the model formulation, it is evident that the virtual temperature effect made significant contributions to the dynamic evolution of the Johnstown MCSs, and its role in future research simulations and/or operational prediction of other MCSs may be substantial. It is important to note, however, that because there is no predictive equation for liquid water in the present model, the hydrostatic loading effect of cloud water on

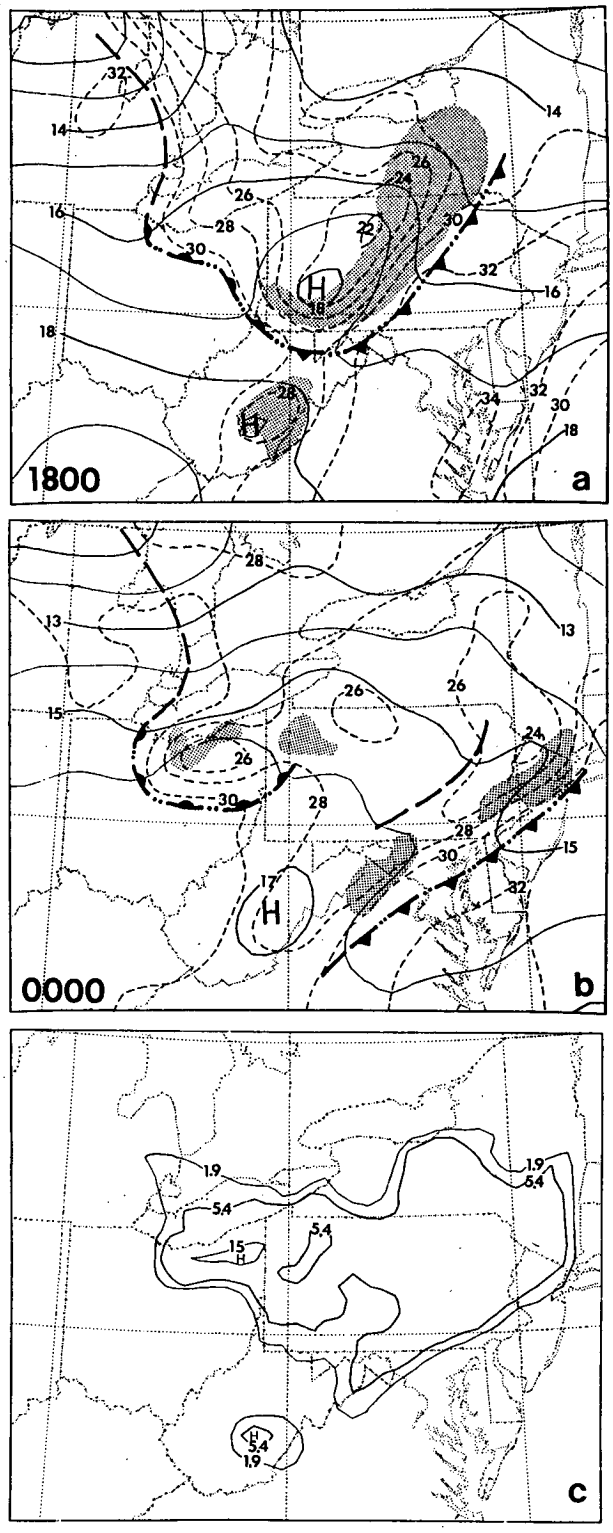

FIG. 19. As in Fig. 7 but for Exp. VTP (virtual temperature).

the gravitational force in computing the geopotential height is neglected. This effect can compensate somewhat for the virtual temperature effect (see Molinari and Dudek, 1986; Zhang et al., 1988). In the Johnstown case, the compensation could be particularly significant for the height gradient around the mesovortex where heavy rainfall occurs.

5. Discussion

It is apparent from the model results that convective and resolvable-scale processes played important yet very different roles in reproducing the individual mesoscale components of the Johnstown MCSs. Specifically, deep convection that occurred prior to the day of the flood was instrumental in creating a mesoscale region of nearly saturated moist adiabatic conditions. The development of new, deep convection in the vicinity of this near-saturated region directly facilitated the production of the squall line, the development of additional deep convection along the boundary of the moist downdraft outflow, and, very importantly, enhanced mesoscale ascent in the near-saturated mesoscale region. This mesoscale ascent resulted in resolvable-scale condensation which further strengthened and deepened the layer of mesoscale convergence and ascent. In this framework, the resolvable-scale condensation could be considered to have been directly responsible for much of the amplification of the major mesolow/warm-core mesovortex. Cloud-scale moist downdrafts acted as a brake on the deepening rate of the vortex by removing moisture that otherwise would be used for the resolvable-scale condensation, and by stabilizing the atmospheric column. In order to understand this evolution of events, many processes must be considered. In the following subsection, we discuss in a dynamical sense how deep convection may be instrumental in the formation of a long-lived midlevel cyclonic circulation (mesolow), an upper-level anticyclonic circulation (mesohigh), and how other factors, particularly moisture, work to produce an inertially-stable warm-core vortex. In subsection b, the stabilizing and destabilizing effects of moist downdrafts are briefly discussed.

a. Genesis of a warm-core mesovortex

As shown by Anthes (1977), the subgrid-scale vertical heating profile from deep convective clouds is primarily determined by two terms, the vertical distribution of latent heat release and the vertical redistribution of sensible heat by the eddy fluxes. Zhang (1985) showed that the FC scheme used for the present study includes these two terms. For environments in which the atmospheric lapse rate is nearly moist adiabatic but still conditionally unstable, the eddy-flux contribution is small and the vertical distribution of latent heat release essentially determines the vertical heating profile. On the other hand, for environments where the midlevel lapse rates are steep (approaching dry adiabatic), the eddy-flux term becomes large and is instrumental in vertically transporting significant amounts of sensible

heat so that upper layers are warmed and low layers are cooled. A diagnostic study by Kuo and Anthes (1984b) indicates a significant contribution of the eddy (sensible and latent heat) flux to the convective heating and moistening profiles. The sensible heat flux does not provide any *net* heating of the atmosphere but simply redistributes heat in a manner that adjusts the atmosphere toward static equilibrium. The redistribution is very similar to the adjustment in a nonprecipitating dry eddy. This implies that the sensible heating by the moist convection tends to warm the same amount of mass at upper levels as that which is cooled at lower levels. The net thermodynamic effect vanishes, but the net dynamic effect does not. The following simple exercise can explain why it does not.

Assume that an amount (ΔP_1) in the lower part of the atmosphere is cooled the same average ($\Delta \bar{T}_1$) as an equivalent amount of mass (ΔP_2) is warmed ($\Delta \bar{T}_2$) at upper levels, i.e.,

$$-\Delta P_1 \cdot \Delta \bar{T}_1 = \Delta P_2 \cdot \Delta \bar{T}_2, \tag{4}$$

where $\Delta \bar{T}_1 = -\Delta \bar{T}_2$, $\Delta P_1 = P_s - P_m = \Delta P_2 = P_m - P_t$, and subscripts s, m and t indicate surface, middle and top levels. The total geopotential height perturbation, $\Delta\Phi'$, can be estimated from the sum of the height changes in the lower and upper levels, i.e.,

$$\begin{aligned}\Delta\Phi' &= \Delta\Phi'_1 + \Delta\Phi'_2 \\ &= -R\Delta\bar{T}_1 \ln\frac{P_m}{P_s} - R\Delta\bar{T}_2 \ln\frac{P_t}{P_m} \\ &= R\Delta\bar{T}_2 \ln(P_m^2/P_sP_t).\end{aligned} \tag{5}$$

Apparently the larger the temperature perturbation and the thicker the layer ($P_s - P_t$) affected by the convection, the stronger the geopotential perturbation. The sensible heating tends to decrease the geopotential heights in the middle and lower parts of the atmosphere and increase the heights above. Note also that temperature changes aloft can produce a much larger effect on the height field than changes introduced at low levels. This suggests that sensible heating and cooling from *deep* convection may have a greater potential for producing dynamic changes (i.e., changes in the mesoscale circulation) than from systems confined to the lower troposphere (see Bolin, 1953; Paegle, 1978).

Consider now the situation where moist downdrafts from deep convection have produced a shallow mesohigh near the surface. Figure 20 schematically depicts the effect of sensible heat redistributions on the shape of the hydrostatic pressure surfaces above the mesohigh. Because of the cold-core temperature perturbation, the mesohigh loses its structure with height and quickly becomes a mesolow with the lowest pressure immediately above the vanishing heating level in the mid-troposphere. Then the reversed temperature gradient caused by the convective warming reduces the strength of the mesolow and eventually produces a strong mesohigh near the tropopause. Adding the effect of latent heating will further strengthen the upper-level high pressure. The response of the atmosphere to the decreasing Φ in low- to midlevels leads to mass convergence while increasing Φ at upper levels causes mass divergence. In particular, strong anticyclonic divergent outflow can develop near the tropopause as indicated by many observations (e.g., Leary, 1979; Fritsch and Maddox, 1981a; Wetzel et al., 1983). From the preceding discussion, it is evident that even when no cloud condensate reaches the ground, as is often seen over semiarid regions, the sensible heat transport by convective clouds may produce significant mesoscale perturbations in horizontal winds. Therefore, it is possible that strong mesoscale circulations may develop even when there is little *net* heating of the atmosphere. This implies that rainfall is not necessarily a good indicator of the magnitude of the impact of deep convection on its environment. Moreover, since the eddy flux contribution is proportional to buoyancy, it is also apparent that explosively developing convective storms have a greater potential for inducing mesoscale circulations than storms with marginally buoyant updrafts, even when the latent heat release is the same. Interestingly, the genesis stage of MCCs is typically characterized by an outbreak of intense and often severe thunderstorms (see Maddox, 1980; 1983).

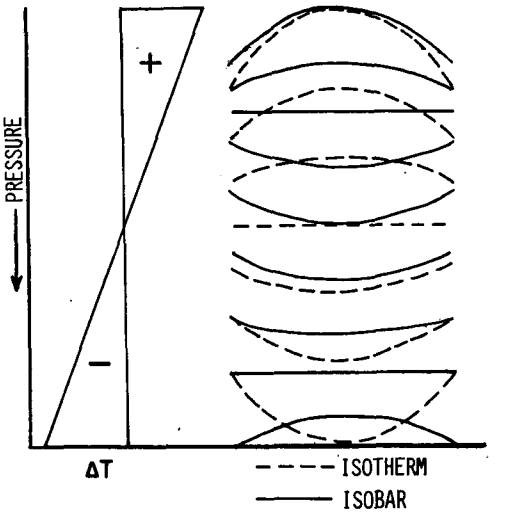

FIG. 20. Schematic diagram showing the effect of sensible heat redistribution on hydrostatic pressure surfaces.

A major problem with making this argument for the genesis of a long-lived mesovortex is that much of the convective heating may be radiated away by outward propagating gravity–inertia waves, and little remains as warming in a *balanced* (hydrostatic, quasi-geostrophic) flow (see Paegle, 1978; Schubert et al., 1980). Furthermore, without mesoscale *saturated* ascent, cooling by adiabatic expansion would tend to quickly offset any residual warming from the deep convection so that the mesoscale circulation would rapidly dimin-

ish as the deep convection dissipated. Still further, horizontal advection, deformation and shear would tend to weaken the concentration of warming necessary for the production of a hydrostatic mesolow. Yet, observations indicate that this is not the case. Specifically, Johnston (1981) used satellite data to document numerous cases where vortices with radii of about 50–100 km emerged from dissipating MCCs. Furthermore, radar studies have repeatedly documented the development of a mesovortex within MCSs (see Houze, 1977; Gamache and Houze, 1982, 1985; Leary and Rappaport, 1987; Smull and Houze, 1985). These vortices sometimes persist for days (see Menard et al., 1986) and can be instrumental in initiating new MCCs on subsequent nights. In the Johnstown MCC case, the remnants of the MCC drifted off the East Coast and developed into a tropical storm (Bosart and Sanders, 1981). Most significantly, however, a mesoanalysis of high-density sounding data in a Pre-STORM event (Johnson, 1986) confirmed the formation of a warm-core vortex. Apparently the loss of energy by gravity–inertia wave outward propagation is either not that great or other factors substantially contribute to the generation of the midlevel mesovortex. Seven such factors come to mind.

1) RAPID MOISTENING OF A MESOSCALE VOLUME

From a hydrostatic and dynamic standpoint, the likelihood of genesis of a long-lived warm-core mesovortex would be considerably enhanced if the *mesoscale* ascent forced by the convective heating became moist adiabatic. Specifically, relative to the surrounding larger-scale environment, the development of a mesoscale moist adiabatic region would tend to produce a localized warm pocket with a corresponding hydrostatic pressure fall. Equally important, the saturated conditions would permit the warm-temperature anomaly to persist in spite of continued mesoscale ascent and adiabatic cooling. Numerous studies have shown that substantial moistening of the mesoscale environment within MCSs is rapidly accomplished by detrainment from deep convective towers (see Houze, 1977; Zipser, 1977; Houze and Chang, 1981; Johnson and Priegnitz, 1981; Johnson and Young, 1983). Apparently, a key factor in the moistening process is that the deep convection *propagates* relative to environmental winds (see Barnes and Sieckman, 1984; Szoke and Zipser, 1986). When a line of deep convection propagates, it leaves in its wake a series of cloud towers and anvils in various stages of decay. This region becomes the well-known "stratiform" regions of MCSs, and it is here that the warm-core mesovortex develops (Gamache and Houze, 1982, 1985; Leary and Rappaport, 1987; Houze and Rappaport, 1984; Smull and Houze, 1985). For a 100–200 km squall line with relative propagation rates on the order of 5–10 m s^{-1}, it is clear that a "stratiform" region comparable in size to the mesovortices can easily be generated in less than 6 hours. Without propagation, lines of convection would not tend to develop "stratiform" areas and would likely continue to exhibit a predominantly two-dimensional line-type structure. This type of distinction between simple line-type structures and more complicated quasi-circular structures is very likely dependent upon thermodynamic and dynamic conditions in the larger-scale environment, e.g., the "ease" with which deep convection can propagate versus the extent to which larger-scale horizontal deformation, shear and vertical motion distort or destroy the stratiform region (see Moncrieff, 1981).

2) VIRTUAL TEMPERATURE EFFECT

The production of a nearly saturated mesoscale region by the propagating deep convection results in a strong horizontal humidity gradient at middle to upper levels (see Ogura and Liou, 1980; Johnson and Preignitz, 1981; Maddox, 1983). Unlike the heating from deep convection, the incorporation of moisture into the atmosphere cannot be quickly propagated away by gravity–inertia waves. Therefore, the virtual temperature effect is more like an actual warming of the atmosphere and will quickly be manifested in the height field through a hydrostatic adjustment. In a study of tropical mesoscale convective systems, LeMone et al. (1984) found a region of hydrostatic pressure deficit in the deep, moist region in the wake of lines of propagating deep convection. For "fast" propagating lines, the pressure fall was on the order of 1 mb which corresponds to about a 10 m height change in the middle to lower troposphere. Correspondingly, for a mean humidity difference of 3 g kg^{-1} in the 600–300 mb layer, the hydrostatic height change is approximately 10 m. Such a height change would be concentrated between the region of saturated mesoscale ascent and the nearby dry ambient environment—a horizontal distance of about 200 km or less. For midlatitudes, this corresponds to about a 5 m s^{-1} adjustment in the geostrophic wind. Since typical environmental wind speeds in the vortex layer are normally less than 15 m s^{-1} and exhibit little vertical shear, 5 m s^{-1} is a significant perturbation to the inertial stability of the vortex (see Zhang and Fritsch, 1987, for additional discussion).

At low levels, humidity gradients can be much stronger than midlevel gradients and tend to be concentrated in elongated zones that parallel the moist ribbons of air feeding the deep convection. As shown in section 4f, the dynamic effects of such gradients are potentially very large, especially in weak-flow summertime situations.

3) AMBIENT VORTICITY

The virtual temperature effect on the height field within the stratiform region may be particularly important during genesis since Schubert et al. (1980), Ooyama (1982), Shapiro and Willoughby (1982), Schubert and Hack (1982) and Hack and Schubert (1986) have shown that heating within a region of relative vorticity larger than the local Coriolis parameter contributes much more efficiently to production of

balanced (vortical) flow than in the situations with little or no positive relative vorticity. The following exercise, while overly simplistic, may nevertheless be helpful in attempting to understand how geopotential height changes and corresponding changes in balanced flow may be *initiated* in MCSs. Specifically, consider that typical convective heating rates in MCSs are on the order of 1° C h^{-1} (Houze, 1982; Johnson and Young, 1983; Kuo and Anthes, 1984a), and that the heating usually occurs for 6 to 12 h. Then, ignoring advection, the *potential* warming is on the order of about 10°C. However, for a midlatitude convective system with a radius of about 100 km and a Rossby deformation radius of 500 km, only about 1% of the heating is manifested as warming (if there is no initial positive relative vorticity in the region of heating); the rest is lost through gravity–inertia waves (see Schubert et al., 1980). The resulting 0.1°C warming in a system's lifetime is considerably less than the observed 0.5 to 3.0°C warming (see Frank, 1978; Ogura and Liou, 1980; Johnson, 1986). However, if the pre-MCC/MCS environment exhibits positive relative vorticity, as is often the case, the gravity-inertia wave energy loss would be less and mesoscale convergence would be more effective at concentrating vorticity. Furthermore, intense midlatitude convective systems have produced heating rates far in excess of 1°C h^{-1}. For example, Ogura and Chen (1977) found heating rates of 5–8°C h^{-1} and Sanders and Paine (1975) computed peak values of 30°C h^{-1}! Therefore, even with the same efficiency (i.e., 1%), these heating rates could easily produce 0.5–3.0°C warmings if they were sustained for only 5 h. Considering that a 1°C warming in the vortex layer (≈600–300 mb) would produce a 20 m height change, and that the observed height perturbations with long-lived midlatitude vortices are about 10 to 40 m, the increase in temperature through the virtual effect, coupled with only a small increase in the energetical efficiency of convective-complex-scale heating in producing balanced vortex flow, could lead to warm-core mesocyclogenesis in weak midlevel flow regimes in midlatitudes. Note though, that since the Rossby deformation radius is considerably larger at low latitudes, much larger areas of convection, or more intense convection, would be required to generate the same geostrophic adjustment at low latitudes than midlatitudes (Schubert et al., 1980; Ooyama, 1982). Thus, *genesis* of mesoscale warm-core vortices may be more likely over some midlatitude land areas than over low-latitude maritime regions, since there is a higher frequency of explosively developing convective systems and associated large heating rates in the midlatitudes. Moreover, high values of relative vorticity associated with traveling disturbances in the westerlies would also enhance the probability of genesis. On the other hand, in many midlatitude situations, large-scale baroclinic processes are much stronger than in the tropics and tend to overwhelm the heat-driven circulations that are favored in weak flow with weak shear. Consequently, it is likely that many midlatitude "attempts" at warm-core mesocyclogenesis are aborted by large-scale deformation and shear before inertial stability is reached.

4) NONLINEAR FEEDBACK

The present study shows that without convective heating and moistening, the mesoscale ascent and stratiform precipitation did not develop (Exp. NPU); it was the feedback among convection, stratiform condensation and mesoscale convergence that had the most effect on the production of the warm-core mesovortex in the model. Therefore, the feedback between deep convection and gravity-inertia-wave convergence (see Hack and Schubert, 1986) may be most important in the sense that the convection causes or enhances mesoscale ascent in the stratiform cloud layer which is the developing warm-core/high-vorticity region. Many investigators (e.g., Leary and Houze, 1979a,b, 1980; Johnson, 1980; Johnson and Young, 1983; Gamache and Houze, 1983; Leary, 1984) have documented the condensation occurring within the stratiform cloud. This "mesoscale condensation" perpetuates the mesoscale moist adiabatic warm-core structure while allowing for mesoscale convergence to spin up the vortex. Furthermore, based upon a radar study by Leary and Rappaport (1987), the "stratiform" region is actually characterized by widespread, marginally unstable convective elements that sometimes become organized into spiral bands. Although this convection is high based and not as deep or intense as that in the original line of thunderstorms, nevertheless it could permit a slight deepening and strengthening of the mesovortex since it provides the potential for additional warming of the "stratiform" region by detrainment of slightly higher θ_e air. Moreover, if the mesoscale convergence and ascent are enhanced, progressively lower-based (higher θ_e) convection is possible since more of the effects of melting, precipitation drag and evaporation would be offset by the stronger upward motion. This results in a deeper and warmer warm core, and therefore a greater mesoscale pressure perturbation.

5) COOLING BY MOIST DOWNDRAFTS

One of the more interesting aspects of the Johnstown warm-core vortex is that it exhibits maximum vorticity between 700 and 500 mb (see Bosart and Sanders, 1981; Zhang and Fritsch, 1987). Based upon Johnston (1981), Menard et al. (1986) and Johnson (1986), the elevated vorticity maximum apparently is typical of such midlatitude warm-core vortices over land. There appears to be several reasons why the level of the vorticity maximum is so high. First, the heating by deep convection and resolvable-scale condensation in a mature MCS tends to maximize above the 500 mb level. Therefore, mesoscale convergence, in response to this heating, tends to maximize around midlevels or even above. Second, cloud-scale penetrative moist downdrafts tend to produce a relatively shallow (typically

<1 km deep) surface-based layer of cool air. Fujita (1959) shows that this cool layer is responsible for the production of mesoscale high-pressure perturbations characterized by *divergent* flow near the surface. This low-level cool air is in a stable structure and is not quickly propagated away by gravity-inertia waves. Rather, the dome of cool air tends to subside and, from continuity, there must be mass convergence above this subsiding, diverging layer. The dissipation of the cool dome seems to be a relatively slow process that continues for 6–18 h (see Maddox and Heckman, 1982). Thus, it may be possible that in weak-flow environments, low to midlevel environmental winds could adjust geostrophically to the presence of low-level domes of cool air. From thermal wind considerations, adjustment to a roughly circular dome of cool air would tend to introduce a cyclonic perturbation above the cold air.

6) RADIATIONALLY DRIVEN OVERTURNING

Using the radiative model of Stephens (1978), Webster and Stephens (1980) demonstrated that within the stratiform cloud region *daytime* radiative effects can be of the same order of magnitude as convective and stratiform condensation heating. Houze (1982) provides a thorough discussion of the implications of Webster and Stephens' results with respect to the vertical circulations of tropical mesoscale convective systems. He points out that the radiative contribution reenforces the condensation heating and enhances the developing mesoscale circulation. It is also possible that radiation contributes favorably to the maintenance and intensification of the mesoscale circulation even after incoming solar radiation ceases. Specifically, it is well established that MCCs in the U.S. are nocturnal (see Maddox, 1980; Maddox et al., 1982; Rodgers et al., 1983, 1985) and reach their maximum extent around 0100–0300 LST. Based upon the calculations of Webster and Stephens (1980), the nocturnal effect of radiation on the thick "stratiform" cloud is to warm the lower half and cool the upper half, thus destabilizing the vertical column. While the net effect is small, the magnitudes of the low-level warming and upper-level cooling are significant (10–15°C day^{-1}), and could initiate or enhance the convective overturning in the stratiform region.

7) MOMENTUM FLUX

Model simulation of the 1977 Johnstown vortex by Zhang and Fritsch (1987) indicates that the momentum transport by resolvable-scale condensation may reduce the vertical shear of the horizontal wind and this is favorable for the rapid generation and maintenance of the warm-core vortex. However, a recent study by LeMone et al. (1984) suggest that the role of the stratiform region in momentum transport is not significant. Note though that the stratiform system they studied was relatively weak in comparison with the vortex-bearing stratiform systems in the midlatitudes.

For the *convective* region, many studies indicate that momentum transport by deep convection significantly influences the general circulation (see review by Moncrieff, 1985). It is interesting though, that in a sensitivity experiment (not shown) where the momentum flux in the convective parameterization was turned off in the Johnstown case, there was no significant difference from the control run. On the other hand, Flatau and Stevens (1987) documented that vertical momentum transports by deep convection can significantly alter horizontal pressure gradients in the vicinity of broad convective lines. Therefore, it is likely that cloud-scale resolution numerical experiments will have to be performed to adequately address the momentum flux problem since valid techniques for transporting momentum (particularly through pressure gradient) in cumulus parameterization schemes have yet to be established.

b. *Moist downdrafts*

Moist downdrafts play an important role in the sensible heat transport. Specifically, moist downdrafts tend to bring low-θ_e air from the midtroposphere into the boundary layer, and thus stabilize the vertical column. This effect is clearly apparent in the comparison of the control simulation to Exp. NPD. Recall that the development of the major mesolow was significantly retarded by the downdrafts. This is a crucial point since the resolution of both operational and research models will very likely increase in the years ahead and therefore the susceptability of these finer-resolution models to spurious deepening of condensation-driven mesolows is also likely to increase.

Although moist downdrafts locally stabilize the atmosphere, they can also initiate and organize convective storms when environmental conditions are conditionally unstable (see Exp. NPU and Simpson, 1980). In particular, moist downdrafts can produce significant mass and wind perturbations that enhance low-level convergence/divergence and produce new convection. In this regard, Purdom (1973) showed that the leading edge of a downdraft-generated mesohigh appeared in satellite imagery as an arc line of convective clouds moving out from an MCS. Purdom (1976) further observed an increase in intensity of individual thunderstorms as they moved across or along a downdraft-generated outflow boundary. Rotunno et al. (1988) documented that downdrafts occurring in an environment with vertical shear enhance upward motion just ahead of gust fronts. In the Johnstown flood case, the numerical results suggest that the cold outflow boundary acted as a quasi-stationary front in which the high-θ_e air from the west overran the downdraft air and produced continued deep convection over western Pennsylvania (see Zhang and Fritsch, 1986a, 1987). Over southern Pennsylvania the cold downdrafts provided direct lifting of boundary layer air for the initiation of convection ahead of the MCC. An additional sensitivity

experiment was conducted (not shown) in which the moist downdrafts were made stronger by artificially decreasing the precipitation efficiency. The results of this experiment showed faster propagation of the squall line and significantly less convection (compared to the control simulation) along the western Pennsylvania border during the evening hours.

6. Summary and concluding remarks

Nine numerical sensitivity simulations were conducted using an 18-h nested-grid simulation of the Johnstown flood MCSs as a control simulation. The results clearly reveal that convective and resolvable-scale heating, moist downdrafts, the diurnal heating cycle, multilevel PBL parameterization and the virtual effect of moisture all have significant effects on the structure, evolution and dynamics of the MCSs. The most important results and conclusions are briefly summarized.

- Diabatic heating plays a crucial role in the generation, amplification and maintenance of mesoscale convective systems and the larger-scale traveling disturbances within which the convective systems develop. The heating provides energy for the deepening of a traveling mesoα-scale short wave, development of strong mesoβ-scale vertical circulations, maintenance of a low-level jet and generation of mesoβ-scale surface pressure perturbations and an upper-level jet streak. Without diabatic heating, all meteorological fields appear to be smoother than that at the initial time, and small (mesoβ) scale features tend to dissipate with time. Thus, whether or not a numerical model can predict the timing and location of the development of MCSs in a weak-gradient environment will have a significant impact not only on the local (mesoβ scale) weather forecast, but also on forecasts of larger-scale patterns, temperature and horizontal winds.
- Development of a warm-core mesolow/mesovortex appears to be closely linked to latent heat release from resolvable-scale ("stratiform") condensation processes. The stratiform condensation can also make an important contribution to the amplification of a short wave and the generation of large-amplitude thermal, pressure and wind perturbations. Although strong penetrative convection contributed about 60%–70% of the total precipitation from the Johnstown MCSs, it is unlikely that it was *directly* responsible for the rapid mesocyclogenesis because the vortex exhibited a saturated warm-core structure which is unfavorable for strong penetrative convection. However, deep convection appears to be important in controlling when and where resolvable-scale condensation may occur and how strong mesocyclogenesis will be. Specifically, deep convection appears to be instrumental in generating a near-saturated and moist adiabatic stratification that permits a positive feedback among low- to midlevel condensation heating, low-level mass and moisture convergence and surface pressure falls. Deep convection can also act in the opposite sense, i.e., "braking" the amplification rate of the cyclogenesis or causing an existing mesolow to fill. In particular, in the present case, after a large area of deep convection intercepted the supply of high-θ_e air to the mesovortex, and replaced it with lower-θ_e downdraft air, the cyclonic circulation and associated stratiform precipitation gradually dissipated. Thus, it appears that numerical prediction of MCSs depends upon the ability of a model to resolve mesoβ-scale time and space variations in convective and resolvable-scale heating profiles. The use of a mean heating profile which is representative of the heating from an entire MCS is unlikely to result in an acceptable prediction of the mesoscale event, particularly the associated rainfall.
- Moist downdrafts have a significant impact on the general evolution of MCSs that develop in weak-gradient environments. This is because downdrafts can produce important low-level perturbations, such as mesohighs, mesotroughs and outflow boundaries, that affect the development of convective storms. On the one hand, the moist downdrafts tend to *stabilize* the atmosphere *vertically* at the place deep convection occurs. On the other hand, downdraft cooling produces horizontal pressure and temperature gradients that, from geostrophic and thermal wind considerations, can enhance the low-level flow into the convective region. Thus, the downdrafts can also result in a *horizontal destabilization* of the environment. The experimental simulations strongly suggest that the cold outflow boundaries over western and southern Pennsylvania played a major role in the development and organization of continued convective activity during evening hours. Thus, it may be necessary to incorporate the downdraft effect into operational (research) models to predict (simulate) the evolution of MCCs and associated quantitative precipitation.
- Inclusion of radiative heating in the surface energy budget tends to generate a conditionally unstable environment favorable for the development and maintenance of deep convection during the daytime. At night, high-θ_e air above the radiatively produced inversion can become an important energy source for the occurrence of overrunning deep convection. Thus, a PBL radiative package is essential for the prediction of the timing and location of convective development. However, it is noteworthy that the omission of the radiative energy had almost the same "braking" effect on the evolution of the mesovortex and associated stratiform precipitation as the moist downdrafts. This suggests that fine-mesh models which include a diurnal heating cycle are susceptible to spurious overdevelopment of mesocyclones unless some type of stabilizing process is introduced. It also suggests that the pronounced diurnal cycle of MCCs may be directly controlled by the heating cycle in the boundary layer.
- Use of the bulk PBL parameterization appears to

have a significant effect on the simulation of the Johnstown MCSs over mountainous regions. The upward energy transport is overestimated on the upwind side of the terrain and underestimated on the downwind side. The results agree with Anthes et al.'s (1980) findings that under horizontally inhomogeneous conditions, the bulk PBL model could not represent the pressure gradient force properly in lower levels. Furthermore, it appears that as the model resolution increases, the simple one-layer PBL formulation is inadequate to represent the vertical fluxes of heat, moisture and momentum over mountainous regions.

- The effects of virtual temperature are to increase parcel buoyancy and alter the horizontal gradients of geopotential height. In late spring and summer seasons, when moisture gradients are very strong and large-scale temperature gradients are weak, the effect of virtual temperature on the height and therefore wind fields can be substantial. In particular, with temperature instead of virtual temperature in the ideal gas law, the model failed to reproduce the major mesolow and MCC.
- The Anthes/Kuo convective scheme is capable of reproducing some mesoβ-scale features (e.g., the squall line) when high resolution is utilized. However, this scheme seems inappropriate to study mesoβ-scale convective systems in weak-gradient but large buoyant-energy situations due to (i) the assumption of moisture convergence and the specification of the "b" parameter to determine latent heating and (ii) the lack of cooling and drying by moist downdrafts. Of course, the present comparative study has some bias toward the use of the Fritsch/Cahppell scheme. Hence, further intercomparison of model simulations using these two schemes is necessary. It is also important to help improve our knowledge of convective parameterization.

In general, the experimental results clearly indicate that the particular treatment of model physics (resolvable or subgrid scale) is very important for forecasting warm-season mesoscale convective weather systems and associated quantitative precipitation. The results also indicate that successful prediction of "convective" weather systems not only hinges upon the convective parameterization, but also upon the concurrent development of the boundary layer and the magnitude and distribution of resolvable-scale latent heat release. Note, however, that the onset and duration of resolvable-scale precipitation are dependent upon the grid resolution, and therefore the size of the grid mesh may also have a significant influence on forecasting success. Although these conclusions are drawn only from one case study, it is possible that many of them may apply to other MCSs that develop in weak-gradient summertime environments.

Finally, when the results of this study are considered together with the results of many other studies of MCSs, the distinguishing dynamical characteristic of an MCC that seems to be emerging is the formation of a warm-core mesovortex in the "stratiform" region. The vortex appears to be a major element in the organization of MCCs and is perhaps the key feature that makes the MCC unique. The formation of a propagating squall line structure could be considered as the initial stage in the atmosphere's attempt to produce the mesovortex, and, under optimal large-scale conditions, the vortex becomes inertially stable. Moreover, in some instances the vortex is instrumental in initiating and organizing new convection that develops into a new MCC (Johnston, 1981) or, in the right large-scale environment, a tropical storm (Velasco and Fritsch, 1987). For most MCCs, however, there is probably an "abortive attempt" to attain inertial stability and only a fraction of the systems succeed. The rest exhibit only a transient warm-core vortical circulation. Nevertheless, this transient circulation is instrumental in helping organize and prolong the life of these circular mesoscale systems.

Acknowledgments. This work was supported by NSF Grant ATM-8418995, USAF AFOSR-83-0064, and the Office of Naval Research SFRC No. N00014-86-K-0688. We are very grateful to R. A. Anthes, Y.-H. Kuo and S. G. Benjamin for their helpful comments. Discussions with W. M. Frank, W. R. Cotton, P. J. Webster, R. A. Houze, G. Holland, L. F. Bosart, J. Brown, F. Sanders, K. Emanuel, J. Molinari, C. Doswell, R. A. Maddox, J. McBride, D. Raymond, C. Leary and E. J. Zipser are gratefully acknowledged. We thank S. Frandsen and D. Corman for skillfully preparing the manuscript. The computations were performed at the National Center for Atmospheric Research which is sponsored by the National Science Foundation.

REFERENCES

Anthes, R. A., 1977: A cumulus parameterization scheme utilizing a one-dimensional cloud model. *Mon. Wea. Rev.*, **105,** 270–286.

——, 1983: Regional models of the atmosphere in middle latitudes. *Mon. Wea. Rev.*, **111,** 1306–1335.

——, 1985: Parameterization of moist convective effects on the thermodynamic and moisture fields in numerical models. *ECMWF Seminar, Phys. Param. Numer. Models Atmos.*, **1,** 121–147.

——, and T. T. Warner, 1978: Development of hydrodynamic models suitable for air pollution and other mesometeorological studies. *Mon. Wea. Rev.*, **106,** 1045–1078.

——, and D. Keyser, 1979: Tests of a fine-mesh model over Europe and the United States. *Mon. Wea. Rev.*, **107,** 963–984.

——, N. L. Seaman and T. T. Warner, 1980: Comparison of numerical simulations of the planetary boundary layer by a mixed-layer and multilayer model. *Mon. Wea. Rev.*, **108,** 365–376.

——, Y.-H. Kuo, S. G. Benjamin and Y.-F. Li, 1982: The evolution of the mesoscale environment of severe local storms: Preliminary modeling results. *Mon. Wea. Rev.*, **110,** 1187–1213.

——, E.-Y. Hsie and Y.-H. Kuo, 1987: Description of the Penn State/NCAR mesoscale model Version 4 (MM4). NCAR Technical Note, NCAR/TN-282+STR, 66 pp.

Barnes, G. M., and K. Sieckman, 1984: The environment of fast- and slow-moving tropical mesoscale convective cloud lines. *Mon. Wea. Rev.*, **112,** 1782–1794.

Benjamin, S. G., and T. N. Carlson, 1986: Some effects of surface heating and topography on the regional severe storm environ-

ment. Part I: Three-dimensional simulations. *Mon. Wea. Rev.*, **114,** 307–329.

Bolin, B., 1953: The adjustment of a nonbalanced velocity field towards geostrophic equilibrium in a stratified fluid. *Tellus,* **5,** 373–385.

Bosart, L. F., 1980: Evaluation of LFM-2 quantitative precipitation forecasts. *Mon. Wea. Rev.*, **108,** 1087–1099.

——, 1981: The Presidents' Day snowstorm of 18–19 February 1979: A subsynoptic-scale event. *Mon. Wea. Rev.*, **109,** 1542–1566.

——, and F. Sanders, 1981: The Johnstown flood of July 1977: A long-lived convective storm. *J. Atmos. Sci.*, **38,** 1616–1642.

Brown, J. M., 1979: Mesoscale unsaturated downdraft driven by rainfall evaporation: A numerical study. *J. Atmos. Sci.*, **36,** 313–338.

Ceselski, B. F., 1973: A comparison of cumulus parameterization techniques. *Tellus,* **25,** 459–478.

Chang, C. B., D. J. Perkey and C. W. Kreitzberg, 1982: A numerical case study of the effects of latent heating on a developing wave cyclone. *J. Atmos. Sci.*, **39,** 1555–1570.

Charba, J. P., and W. H. Klein, 1980: Skill in precipitation forecasting in the National Weather Service. *Bull. Amer. Meteor. Soc.*, **61,** 1546–1555.

Cotton, W. R., R. L. George, P. J. Wetzel and R. L. McAnelly, 1983: A long-lived mesoscale convective complex. Part I: The mountain-generated component. *Mon. Wea. Rev.*, **111,** 1893–1918.

Doneaud, A. A., J. R. Miller, Jr., D. L. Priegnitz and L. Viswanath, 1983: Surface mesoscale features as potential storm predictors in the Northern Great Plains—two case studies. *Mon. Wea. Rev.*, **111,** 273–292.

Eom, J., 1975: Analysis of the internal gravity wave occurrence of 19 April 1970 in the Midwest. *Mon. Wea. Rev.*, **103,** 217–226.

Flatau, M., and D. E. Stevens, 1987: The effect of horizontal pressure gradients on the momentum transport in tropical convective lines. Part I: The results of the convective parameterization. *J. Atmos. Sci.*, **44,** 2074–2087.

Frank, W. M., 1978: The life cycles of GATE convective systems. *J. Atmos. Sci.*, **35,** 1256–1264.

Fritsch, J. M., 1986: *Precipitation Enhancement—A Scientific Challenge.* Chap. 8: Modification of mesoscale convective weather systems. *Meteor. Monogr.*, No. 43, Amer. Meteor. Soc., 77–86.

——, and C. F. Chappell, 1980: Numerical prediction of convectively driven mesoscale pressure systems. Part I: Convective parameterization. *J. Atmos. Sci.*, **37,** 1722–1733.

——, and R. A. Maddox, 1981a: Convectively driven mesoscale pressure systems aloft. Part I: Observations. *J. Appl. Meteor.*, **20,** 9–19.

——, and ——, 1981b: Convectively driven mesoscale weather systems aloft. Part II: Numerical simulations. *J. Appl. Meteor.*, **20,** 20–26.

——, C. F. Chappell and L. R. Hoxit, 1976: The use of large-scale budgets for convective parameterization. *Mon. Wea. Rev.*, **104,** 1408–1418.

Fujita, T., 1959: Precipitation and cold-air production in mesoscale thunderstorm systems. *J. Meteor.*, **16,** 454–466.

Gamache, J. F., and R. A. Houze, 1982: Mesoscale air motions associated with a tropical squall line. *Mon. Wea. Rev.*, **110,** 118–135.

——, and ——, 1983: Water budget of a mesoscale convective system in the tropics. *J. Atmos. Sci.*, **40,** 1835–1850.

——, and ——, 1985: Further analysis of the composite wind and thermodynamic structure of the 12 September GATE squall line. *Mon. Wea. Rev.*, **113,** 1241–1259.

Garrett, A. J., 1982: A parameter study of interactions between convective clouds, the convective boundary layer, and a forested surface. *Mon. Wea. Rev.*, **110,** 1041–1059.

Gauntlett, D. J., L. M. Leslie, J. L. McGregor and D. R. Hincksman, 1978: A limited area nested numerical weather prediction model: Formulation and preliminary results. *Quart. J. Roy. Meteor. Soc.*, **104,** 103–117.

Gray, W. M., 1973: Cumulus convection and large-scale circulations. I: Broadscale and mesoscale considerations. *Mon. Wea. Rev.*, **101,** 839–853.

Gyakum, J. R., 1983: On the evolution of the *QE II* storm. II: Dynamic and thermodynamic structure. *Mon. Wea. Rev.*, **111,** 1156–1173.

Hack, J. J., and W. H. Schubert, 1986: Nonlinear response of atmospheric vortices to heating by organized cumulus convection. *J. Atmos. Sci.*, **43,** 1559–1573.

Heideman, K. F., 1986: On the warm-season quantitative precipitation forecast problem. M.S. thesis, Department of Meteorology, The Pennsylvania State University, 96 pp.

Houze, R. A., Jr., 1977: Structure and dynamics of a tropical squall-line system. *Mon. Wea. Rev.*, **105,** 1540–1567.

——, 1982: Cloud clusters and large-scale vertical motions in the tropics. *J. Meteor. Soc. Japan,* **60,** 396–409.

——, and C.-P. Chang, 1981: Inclusion of mesoscale updrafts and downdrafts in computations of vertical fluxes by ensembles of tropical clouds. *J. Atmos. Sci.*, **38,** 1751–1770.

——, and E. N. Rappaport, 1984: Air motions and precipitation structure of an early summer squall line over the eastern tropical Atlantic. *J. Atmos. Sci.*, **41,** 553–574.

Hoxit, L. R., R. A. Maddox, C. F. Chappell, F. L. Zuckerberg, H. M. Mogil, I. Jones, D. R. Greene, R. E. Saffle and R. A. Scofield, 1978: Meteorological analysis of the Johnstown, Pennsylvania flash flood, 19–20 July 1977. NOAA Tech. Rep. ERL 401-APCL 43. 71 pp.

Johnson, R. H., 1976: The role of convective-scale precipitation downdrafts in cumulus and synoptic-scale interactions. *J. Atmos. Sci.*, **33,** 1890–1910.

——, 1980: Diagnosis of convective and mesoscale motions during Phase III of GATE. *J. Atmos. Sci.*, **37,** 733–753.

——, 1984: Partitioning tropical heat and moisture budgets into cumulus and mesoscale components: Implications for cumulus parameterization. *Mon. Wea. Rev.*, **112,** 1590–1601.

——, 1986: The development of organized mesoscale circulations within Oklahoma-Kansas Pre-STORM convective systems. *Preprints, Int. Conf. on Monsoon and Mesoscale Meteorology,* Taiwan, 100–104.

——, and D. L. Priegnitz, 1981: Winter monsoon convection in the vicinity of North Borneo. Part II: Effects on large-scale fields. *Mon. Wea. Rev.*, **109,** 1615–1628.

——, and G. S. Young, 1983: Heat and moisture budgets of tropical mesoscale anvil clouds. *J. Atmos. Sci.*, **40,** 2138–2147.

Johnston, E. C., 1981: Mesoscale vorticity centers induced by mesoscale convective complexes. M.S. thesis, University of Wisconsin, 54 pp.

Jones, R. W., 1977: A nested grid for a three-dimensional model of a tropical cyclone. *J. Atmos. Sci.*, **34,** 1528–1553.

Kalb, M. W., 1987: The role of convective parameterizations in the simulation of a Gulf Coast precipitation system. *Mon. Wea. Rev.*, **115,** 214–234.

Kasahara, A., 1961: A numerical experiment on the development of a tropical cyclone. *J. Meteor.*, **18,** 269–282.

Keyser, D., and R. A. Anthes, 1982: The influence of planetary boundary layer physics on frontal structure in the Hoskins-Bretherton horizontal shear model. *J. Atmos. Sci.*, **39,** 1783–1802.

Koss, W. J., 1976: Linear stability analysis of CISK-induced disturbances: Fourier component eigenvalue analysis. *J. Atmos. Sci.*, **33,** 1195–1222.

Kreitzberg, C. W., and D. J. Perkey, 1976: Release of potential instability: Part I: A sequential plume model within a hydrostatic primitive equation model. *J. Atmos. Sci.*, **33,** 456–475.

——, and ——, 1977: Release of potential instability: Part II: The mechanisms of convective/mesoscale interaction. *J. Atmos. Sci.*, **34,** 1569–1595.

Krishnamurti, T. N., 1985: Numerical weather prediction in low latitudes. *Advances in Geophysics,* Vol. 28, Academic Press, 283–333.

Kuo, H. L., 1974: Further studies of the parameterization of the

influence of cumulus convection on large-scale flow. *J. Atmos. Sci.*, **31**, 1232–1240.

Kuo, Y.-H., and R. A. Anthes, 1984a: Mesoscale budgets of heat and moisture in a convective system over the central United States. *Mon. Wea. Rev.*, **112**, 1482–1497.

——, and ——, 1984b: Semiprognostic tests of Kuo-type cumulus parameterization schemes in an extratropical convective system. *Mon. Wea. Rev.*, **112**, 1498–1509.

Kurihara, Y., and M. A. Bender, 1980: Use of a movable nested-mesh model for tracking a small vortex. *Mon. Wea. Rev.*, **118**, 1782–1809.

Lakhtakia, M., and T. T. Warner, 1987: A real-data numerical study of the development of the precipitation along the edge of an elevated mixed layer. *Mon. Wea. Rev.*, **115**, 156–168.

Leary, C. A., 1979: Behavior of the wind field in the vicinity of a cloud cluster in the intertropical convergence zone. *J. Atmos. Sci.*, **36**, 631–639.

——, 1980: Temperature and humidity profiles in mesoscale unsaturated downdrafts. *J. Atmos. Sci.*, **37**, 1005–1012.

——, 1984: Precipitation structure of the cloud clusters in a tropical easterly wave. *Mon. Wea. Rev.*, **112**, 313–325.

——, and R. A. Houze, 1979a: The structure and evolution of convection in a tropical cloud cluster, *J. Atmos. Sci.*, **36**, 437–457.

——, and ——, 1979b: Melting and evaporation of hydrometers in precipitation from the anvil clouds of deep tropical convection. *J. Atmos. Sci.*, **36**, 669–679.

——, and ——, 1980: The contribution of mesoscale motions to the mass and heat fluxes of an intense tropical convective system. *J. Atmos. Sci.*, **37**, 784–796.

——, and E. N. Rappaport, 1987: The life cycle and internal structure of a mesoscale convective complex. *Mon. Wea. Rev.*, **115**, 1503–1527.

LeMone, M. A., G. M. Barnes and E. J. Zipser, 1984: Momentum flux by lines of cumulonimbus over the tropical oceans. *J. Atmos. Sci.*, **41**, 1914–1932.

Lewis, J. M., 1975: Test of Ogura-Cho model on a prefrontal squall line case. *Mon. Wea. Rev.*, **103**, 764–778.

Lopez, R. E., 1973: A parametric model of cumulus convection. *J. Atmos. Sci.*, **30**, 1354–1373.

Maddox, R. A., 1980: Mesoscale convective complexes. *Bull. Amer. Meteor. Soc.*, **61**, 1374–1387.

——, 1983: Large-scale meteorological conditions associated with midlatitude, mesoscale convective complexes. *Mon. Wea. Rev.*, **111**, 1475–1493.

——, and B. E. Heckman, 1982: The impact of mesoscale convective weather systems upon MOS temperature guidance. *Proc. Ninth Conf. on Wea. Forecasting and Analysis*, Seattle, Amer. Meteor. Soc., 214–218.

——, L. R. Hoxit and C. F. Chappell, 1980: A study of tornadic thunderstorm interactions with thermal boundaries. *Mon. Wea. Rev.*, **108**, 322–336.

——, D. J. Perkey and J. M. Fritsch, 1981: Evolution of upper tropospheric features during the development of a mesoscale convective complex. *J. Atmos. Sci.*, **38**, 1664–1674.

——, D. M. Rodgers and K. W. Howard, 1982: Mesoscale convective complexes over the United States during 1981—Annual Summary. *Mon. Wea. Rev.*, **110**, 1501–1514.

Mahrer, Y., and R. A. Peilke, 1977: The effects of topography on sea and land breezes in a two-dimensional numerical model. *Mon. Wea. Rev.*, **105**, 1151–1162.

Menard, R., J. Merritt, J. M. Fritsch and P. Hirschberg, 1986: Mesoanalysis of a convectively-generated inertially stable mesovortex. *Preprints, 11th Conf. Weather Forecasting and Analysis.* Kansas City, Amer. Metor. Soc., 194–199.

Molinari, J., and T. Corsetti, 1985: Incorporation of cloud-scale and mesoscale downdrafts into a cumulus parameterization: Results of one- and three-dimensional integrations. *Mon. Wea. Rev.*, **113**, 485–501.

——, and M. Dudek, 1986: Implicit versus explicit convective heating in numerical weather prediction models. *Mon. Wea. Rev.*, **114**, 1822–1831.

Moncrieff, M. W., 1981: A theory of organized steady convection and its transport properties. *Quart. J. Roy. Meteor. Soc.*, **107**, 29–50.

——, 1985: Convective momentum transport. *ECMWF Seminar, Phys. Param. Numer. Models Atmos.*, **1**, 181–203.

Ninomiya, K., 1971a: Mesoscale modification of synoptical situations from thunderstorm development as revealed by ATS III and aerological data. *J. Appl. Meteor.*, **10**, 1103–1121.

——, 1971b: Dynamical analysis of outflow from tornado-producing thunderstorms as revealed by ATS III pictures. *J. Appl. Meteor.*, **10**, 778–798.

Ogura, Y., and H. R. Cho, 1973: Diagnostic determination of cumulus cloud populations from observed large-scale variables. *J. Atmos. Sci.*, **30**, 1276–1286.

——, and Y.-L. Chen, 1977: A life history of an intense mesoscale convective storm in Oklahoma. *J. Atmos. Sci.*, **33**, 1458–1476.

——, and M. T. Liou, 1980: The structure of a midlatitude squall line: A case study. *J. Atmos. Sci.*, **37**, 553–567.

——, and J.-Y. Jiang, 1985: A modeling study of heating and drying effects of convective clouds in an extratropical mesoscale convective system. *J. Atmos. Sci.*, **42**, 2478–2492.

Ooyama, K., 1982: Conceptual evolution of the theory and modeling of the tropical cyclone. *J. Meteor. Soc. Japan*, **60**, 369–379.

Paegle, J., 1978: The transient mass-flow adjustment of heated atmospheric circulations. *J. Atmos. Sci.*, **35**, 1678–1688.

Perkey, D. J., and R. A. Maddox, 1985: A numerical investigation of a mesoscale convective system. *Mon. Wea. Rev.*, **113**, 553–566.

Pielke, R. A., 1984: *Mesoscale Meteorological Modeling.* Academic Press. 612 pp.

Purdom, J. F. W., 1973: Mesohighs and satellite imagery. *Mon. Wea. Rev.*, **101**, 180–181.

——, 1976: Some uses of high-resolution GOES imagery in the mesoscale forecasting of convection and its behavior. *Mon. Wea. Rev.*, **104**, 1474–1483.

Rockwood, A. A., D. L. Bartels and R. A. Maddox, 1984: Precipitation characteristics of a dual mesoscale convective complex. NOAA Tech. Rep. ERL ESG-6, 50 pp.

Rodgers, D. M., K. W. Howard and E. C. Johnston, 1983: Mesoscale convective complexes over the United States during 1982. *Mon. Wea. Rev.*, **111**, 2363–2369.

——, M. J. Magnano and J. H. Arns, 1985: Mesoscale convective complexes over the United States during 1983. *Mon. Wea. Rev.*, **113**, 888–901.

Rosenthal, S. L., 1979: The sensitivity of simulated hurricane development to cumulus parameterization details. *Mon. Wea. Rev.*, **107**, 193–197.

Rotunno, R., J. B. Klemp and M. Weisman, 1988: A theory for strong, long-lived squall lines. *J. Atmos. Sci.*, in press.

Sanders, F., 1979: Trends in skill of daily forecast of temperature and precipitation, 1966–78. *Bull. Amer. Meteor. Soc.*, **60**, 763–769.

——, and R. J. Paine, 1975: The structure and thermodynamics of an intense mesoscale convective storm in Oklahoma. *J. Atmos. Sci.*, **32**, 1563–1579.

——, and J. R. Gyakum, 1980: Synoptic-dynamic climatology of the "bomb". *Mon. Wea. Rev.*, **108**, 1589–1606.

Sardie, J. M., and T. T. Warner, 1983: On the mechanism for the development of polar lows. *J. Atmos. Sci.*, **40**, 869–881.

Schubert, W. H., and J. J. Hack, 1982: Inertial stability and tropical cyclone development. *J. Atmos. Sci.*, **39**, 1687–1697.

——, ——, P. L. Silva Dias and S. R. Fulton, 1980: Geostrophic adjustment in an axisymmetric vortex. *J. Atmos. Sci.*, **37**, 1464–1484.

Shapiro, L. J., and H. E. Willoughby, 1982: The response of balance hurricanes to local sources of heat and momentum. *J. Atmos. Sci.*, **39**, 378–394.

Simpson, J., 1980: Downdrafts as linkages in dynamic cumulus seeding effects. *J. Appl. Meteor.*, **19**, 477–487.

Smull, B. F., and R. A. Houze, Jr., 1985: A midlatitude squall line

with a trailing region of stratiform rain: Radar and satellite observations. *Mon. Wea. Rev.*, **113,** 117–133.

Stephens, G. L., 1978: Radiative properties of extended water clouds, Part I. *J. Atmos. Sci.*, **35,** 2111–2122.

Szoke, E. J., and E. J. Zipser, 1986: A radar study of convective cells in mesoscale systems in GATE. Part II: life cycles of convective cells. *J. Atmos. Sci.*, **43,** 199–218.

Tracton, M. S., 1973: The role of cumulus convection in the development of extratropical cyclones. *Mon. Wea. Rev.*, **101,** 573–593.

Uccellini, L. W., 1975: A case study of apparent gravity wave initiation of severe convective storms. *Mon. Wea. Rev.*, **103,** 497–513.

Velasco, I., and J. M. Fritsch, 1987 : Mesoscale convective complexes in the Americas. *J. Geophys. Res.*, **92,** 9591–9613.

Webster, P. J., and G. L. Stephens, 1980: Tropical upper-tropospheric extended clouds: Inferences from winter MONEX. *J. Atmos. Sci.*, **37,** 1521–1541.

Wetzel, P. J., W. R. Cotton and R. L. McAnelly, 1983: A long-lived mesoscale convective complex. Part II. Evolution and structure of the mature complex. *Mon. Wea. Rev.*, **111,** 1919–1937.

Zack, J. W., M. L. Kaplan and V. C. Wong, 1985: A comparison of the prognostic performance of several parameterizations in mesoscale simulations of the 10 April 1979 SESAME I case. *Seventh Conf. on Numerical Weather Prediction.*, Amer. Meteor. Soc., 415–422.

Zhang, D.-L., 1985: Nested-grid simulation of the mesoβ scale structure and evolution of the Johnstown flood of July 1977. Ph.D. dissertation, The Pennsylvania State University, 270 pp.

——, and R. A. Anthes, 1982: A high-resolution model of the planetary boundary layer-sensitivity tests and comparison with SESAME-79 data. *J. Appl. Meteor.*, **21,** 1594–1609.

——, and J. M. Fritsch, 1986a: Numerical simulation of the meso-β scale structure and evolution of the 1977 Johnstown flood. Part I: Model description and verification. *J. Atmos. Sci.*, **43,** 1913–1943.

——, and ——, 1986b: A case study of the sensitivity of numerical simulation of mesoscale convective systems to varying initial conditions. *Mon. Wea. Rev.*, **114,** 2418–2431.

——, and ——, 1987: Numerical simulation of the mesoβ scale structure and evolution of the 1977 Johnstown flood. Part II: Inertially stable warm-core vortex and the mesoscale convective complex. *J. Atmos. Sci.*, **44,** 2593–2612.

——, H.-R. Chang, N. L. Seaman, T. T. Warner and J. M. Fritsch, 1986: A two-way interactive nesting procedure with variable terrain resolution. *Mon. Wea. Rev.*, **114,** 1330–1339.

——, E.-Y. Hsie and M. W. Moncrieff, 1988: A comparison of explicit and implicit predictions of convective and stratiform precipitating weather systems with a mesoβ scale numerical model. *Quart. J. Roy. Meteor. Soc.*, **114,** 31–60.

Zipser, E. J., 1977: Mesoscale and convective-scale downdrafts as distinct components of squall-line circulation. *Mon. Wea. Rev.*, **105,** 1568–1589.